Preprints.org

Review

Not peer-reviewed version

Trends in Photothermal Nanostructures for Antimicrobial Applications

Violeta Dediu , Jana Ghitman , Gratiela Gradisteanu-Pircalabioru , Kiat Hwa Chan , Florina Silvia Iliescu * , Ciprian Iliescu *

Posted Date: 16 May 2023

doi: 10.20944/preprints202305.1106.v1

Keywords: photothermal-antimicrobials; antibacterial mechanisms; anti-biofilm; wound healing

Preprints.org is a free multidiscipline platform providing preprint service that is dedicated to making early versions of research outputs permanently available and citable. Preprints posted at Preprints.org appear in Web of Science, Crossref, Google Scholar, Scilit, Europe PMC.

Copyright: This is an open access article distributed under the Creative Commons Attribution License which permits unrestricted use, distribution, and reproduction in any medium, provided the original work is properly cited.

Preprints (www.preprints.org) | NOT PEER-REVIEWED | Posted: 16 May 2023 doi:10.20944/preprints202305.1106.v1

Disclaimer/Publisher's Note: The statements, opinions, and data contained in all publications are solely those of the individual author(s) and contributor(s) and not of MDPI and/or the editor(s). MDPI and/or the editor(s) disclaim responsibility for any injury to people or property resulting from any ideas, methods, instructions, or products referred to in the content.

Review

Trends in Photothermal Nanostructures for Antimicrobial Applications

Violeta Dediu [1], Jana Ghitman [2,3], Gratiela Gradisteanu-Pircalabioru [2,6,7], Kiat Hwa Chan [4,5], Florina Silvia Iliescu [1,*] and Ciprian Iliescu [1,2,6,*]

1. National Research and Development Institute in Microtechnologies – IMT Bucharest, 126A Erou Iancu Nicolae Street, 077190 Voluntari, Romania; violeta.dediu@imt.ro; (V.D); florina.iliescu@imt.ro (F.S.I.)
2. eBio-hub Research-Center, University "Politehnica" of Bucharest, 6 Iuliu Maniu Bulevard, Campus Building, Bucharest 061344, Romania, ggradisteanu@upb.ro;(G.G.P.) ciprian.iliescu@upb.ro (C.I.)
3. Advanced Polymer Materials Group, University Politehnica of Bucharest, 1-7 Gh. Polizu Street 011061 Bucharest, Romania; jana.ghitman@upb.ro (J.G.)
4. Division of Science, Yale-NUS College, 16 College Avenue West, Singapore 138527;
5. NUS College, National University of Singapore, 18 College Avenue East, Singapore 138593kiathwa.chan@yale-nus.edu.sg
6. Academy of Romanian Scientists, 54 Splaiul Independentei, 050094 Bucharest, Romania
7. Research Institute of University of Bucharest, University of Bucharest, 050095, Bucharest, Romania

* Correspondence: florina.iliescu@imt.ro (F.S.I) ciprian.iliescu@upb.ro (C.I.);

Abstract: Rapid developing antimicrobial resistance due to broad antibiotic utilisation in healthcare and food industries and the non-availability of novel antibiotics represents one of the most critical public health issues worldwide. The current advances in nanotechnology allow new materials to address drug-resistant bacterial infections in specific, focused and biologically safe ways. The unique physicochemical properties, biocompatibility, and wide range of adaptability of nanomaterials that exhibit photothermal capability can be employed to develop the next generation of photothermally induced controllable hyperthermia as antibacterial nanoplatforms. Here, we review the current state-of-the-art in different functional classes of photothermal antibacterial nanomaterials and the strategies to optimise antimicrobial efficiency. The recent achievements and trends in developing photothermally active nanostructures, including plasmonic metals, semiconductor, carbon-based, and organic photothermal polymers, and antibacterial mechanisms of action, including anti-multidrug resistant bacteria and biofilms removal, will be discussed. Insights into mechanisms of the photothermal effect and various factors influencing photothermal antimicrobial performance, emphasising the structure–performance relationship, are discussed. We will examine the photothermal agents' functionalisation for specific bacteria, effects of near-infrared light irradiation spectrum, or active photothermal materials for multimodal synergistic-based therapies to minimise side effects and maintain low cost. Most relevant applications are presented, such as anti-biofilm formation, biofilm penetration or ablation, and nanomaterial-based infected wound therapy. Practical antibacterial applications employing the photothermal antimicrobial agents, alone or in synergistic combination with other nanomaterials, are considered. Existing challenges and limitations in photothermal antimicrobial therapy and future perspectives are presented from the structure, function, safety, and clinical potential points of view.

Keywords: photothermal-antimicrobials; antibacterial mechanisms; anti-biofilm; wound healing

1. Introduction

Bacterial infections and related antimicrobial resistance are under World health Organisation (WHO) and Centers of Disease Control and Prevention (CDC) surveillance worldwide,[1] in all healthcare sectors and agriculture,[2] due to the increased morbidity and mortality caused.[3] Increasing antimicrobial resistance is one of the top ten "global public health threats facing

© 2023 by the author(s). Distributed under a Creative Commons CC BY license.

Preprints (www.preprints.org) | NOT PEER-REVIEWED | Posted: 16 May 2023 doi:10.20944/preprints202305.1106.v1

humanity", [4,5] thus impacting individuals at every stage of life, personal, professional levels or societal.[6,7] Bacteria are harmful to humans directly through the resistance to commonly used antibiotics [8] or the resulting severe adverse effects induced by the second and third-line treatments of nosocomial infections, primarly antibiotic-resistant infections.[4,6,9–13] One of the most pressing challenges is to define new antibacterial materials and strategies with high efficiency, safety, and convenience,[14] knowing that traditional drugs or methods failed due to drug resistance.[15,16] Nanotechnology-based delivery systems and engineered nanoparticles developed as alternative "nanoantibiotics".[17] Nanoparticles (NPs) demonstrated the most effective method to address multi-drug-resistant bacteria since they not only act as transporters for natural antibiotics and antimicrobials but also actively combat bacteria. Inorganic NPs (e.g., silver (Ag), [18–21] zinc oxide (ZnO) [22–24], gold (Au) [25–27], titanium oxide TiO_2 [28], copper (Cu)[29], copper oxide (CuO) [30], Nickel (Ni), [31] selenium (Se)),[32] and natural and synthetic organic NPs (e.g., liposomes, polymeric nanoparticles, micelles, ferritin), [33,34] can be used alone or as nanocarriers for therapeutic molecules (e.g., liposomes, polymeric NPs, and dendrimers).[35,36] Hybrid NPs combine organic and inorganic NPs in the same composite system.[37] Nanomaterials were used as antibacterial agents, and dynamic therapies were designed for better efficacy by increasing drugs' bioavailability, targeted distribution, and decreasing toxicity.[38–40] Notably, the nanomaterials' physical and chemical properties (dimension under 100 nm, morphology, crystal structure, defect state, surface energy, surface potential) can be tuned to meet the requirements of specific applications.[41,42] Moreover, stimulus-based tuneable noninvasive approaches include dynamic therapy, which employs various stimuli such as thermal (photothermal therapy),[43] chemical or electrical [44] (photodynamic therapy - PDT), immunotherapy,[45] and gene therapy, each of them with their advantages and limitations.[17,46,47] In the case of localised surface plasmon resonance (LSPR) by photothermally active nanomaterials (photothermal agents - PTAs), the absorbed energy (near-infrared -NIR- light, 700-1300 nm) is released as heat (hyperthermia up to 90 °C). It alters the membrane, inactivates proteins, and releases intracellular material for *in situ*-fine-tuning photothermal ablation of bacteria or even damaging surrounding cells.[46] The photothermal effect, in range with the *biological transparency window*,[48] allows deep penetration of light (up to 1cm) into infected tissue,[49] avoids mutations in the targeted bacteria and kills planktonic multidrug-resistant (MDR) microorganisms and biofilm. However, the short and long-term biological concerns restricting PTT applications imposed PTAs functionalisation for specific bacteria, moving towards lower-energy (i.e.., NIR-II 1000–1700 nm, and NIR-III 1800–2100 nm) or active photothermal materials for multimodal synergistic-based therapies to minimize side effects and maintain low cost (i.e., PTT-PDT, PTT- CDT, PTT-photocatalytic, PTT-immunotherapy, PTT-catalytic).[50,51]

Here, we review the recent achievements and current trends in developing photothermally active nanostructures, including plasmonic metals, semiconductor, carbon-based, and organic photothermal polymers, and antibacterial mechanisms of action (MOA), including anti-MDR bacteria and biofilms removal. Also, new non-conventional photothermal-based antimicrobial systems with remarkable synergistic effects are presented. Most relevant PTAs applications are reviewed, such as anti-biofilm formation, biofilm penetration or ablation, and nanomaterial-based infected wound therapy. We overview the strength, limitations, and general challenges of photothermal treatment using nanomaterials to highlight the research directions.

2. Photothermal antimicrobial mechanism

When subjected to heating at temperatures above 45°C, most bacteria viability is altered the PTAs used, different mechanisms of photothermal conversion can occur: the localized surface plasmon resonance in metals, electron-hole generation and relaxation of semiconductors, and HOMO (highest occupied molecular orbital)–LUMO (lowest unoccupied molecular orbital) excitation and lattice vibration of molecules.[52]

Preprints (www.preprints.org) | NOT PEER-REVIEWED | Posted: 16 May 2023 doi:10.20944/preprints202305.1106.v1

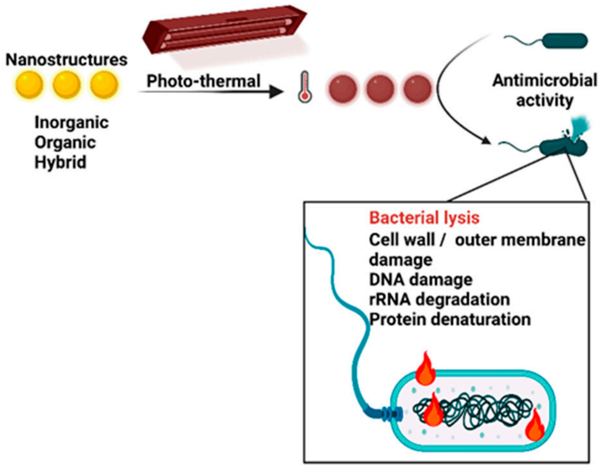

Figure 1. Schematic photothermal antimicrobial mechanism of PTAs nanostructures.

The metal NPs' photothermal antibacterial action relies on the absorption of visible light radiation with plasmon formation (collective oscillation of conduction electrons) followed by a high-speed transfer of the generated heat to the surrounding bacteria inducing cell/bacteria death. The outcomes of the photothermal bacteria ablation depend on the NPs size, shape, and dielectric constant and surrounding materials' permittivity, incident light wavelength, and its intensity. These parameters can be tuned for the optimisation of the photothermal interactions.[53] Semiconductors act through the generation and relaxation of electron-hole pairs after irradiation by incident light with an energy similar to the band gap.[54] Carbon and polymer-based materials generate a photothermal effect through the lattice vibration of molecules. Upon illumination with light energy, the excited electron goes from the ground state (LUMO) to a higher energy orbital (HOMO)). Next, electron-phonon coupling enables the relaxation from the higher excitation states to the lower energy states. Hence, the energy gained is conveyed from the excited electrons to the vibrational modes within the atomic lattices, triggering an increased temperature.[54,55] The photothermal action cannot be isolated from other ways of antimicrobial action, such as nanoperforation, destruction of membrane stability, biomolecule binding, and oxidative damage.[56] These interactions between NPs and bacteria depend on many factors, such as NP's surface chemistry, charge and hydrophobicity. Photothermal action mainly depends on dielectric constants of PTAs nanoparticles and surrounding materials.

3. Photothermal antimicrobials agents

Metals (such as Au, Cu, Pd, Bi), semiconductors oxide (WO_3, Fe_3O_4), semiconductors chalcogenides or dichalcogenides (CuS, MoS_2, NiS_2, SnSe, CuSe), mettaloids (B) and nonmetals (C, P) are inorganic nanostructures that absorb energy strongly in the NIR region.

Metal-based NPs are at the forefront of fighting bacteria as" light-directed nanoheaters" due to their substantial light-to-heat conversion efficiency. Recent achievements focused on developing plasmonic metals have boosted their applications in antimicrobial applications. Plasmonic metal NPs can express an effective and targeted antibacterial activity against a broad spectrum of bacterial strains.

The most used plasmonic metal for bacteria photothermolysis is Au in different shapes, sizes, and structures. The representative Au-based PTAs, and other inorganic nanomaterials and their antibacterial activities are presented in Table 1. Nano-gold (nanorods, nanostars, nanobipyramids, nanowires, nanoworms, nanoflowers) present fascinating localised surface plasmonic resonance (LSPR) properties while the chemical inertness that makes gold nanostructures suitable for bacteria ablation through photoinduced hyperthermia. Au NPs have been widely adopted for biological applications due to their easy nanoscale fabrication and high oxidation and degeneration

Preprints (www.preprints.org) | NOT PEER-REVIEWED | Posted: 16 May 2023 doi:10.20944/preprints202305.1106.v1

resistance.[57] Controlling the shape and size of Au nanostructures, optically tuned the LSPR activity, at different light wavelengths, from visible to the NIR region.[58,59] Using Au NPs for bacterial photothermal ablation is an evolving application, from the first *in vitro* study using bioconjugated Au plasmonic NPs under laser light [60] to the proof of principle of PTT biofilm removing [61] and Au nanostructures involved in PTT bacteria ablation.[62,63] Au nanorods (Au NRs) were the most utilised because of their longitudinal surface plasmon resonances under NIR laser illumination. In the case of Au NRs, the photothermal bacteria ablation efficiency depends on the Au nanocrystals' shape, size, overall structure, and, most importantly, their facets. Yougbare *et al.* compared Au NRs with the (200) plane and Au nanobipyramids (Au NBPs) with the (111) plane and found that the photothermal activity of Au NBPs (111) was better against *E. coli* due to easy desorbed water on the Au NBPs (111) surface for PTT hyperthermia.[64] However, the pulsed laser irradiation induces structural damage and shape modification on Au NRs.[65,66] imposing additional treatment to improve structural stability under laser treatment.[40] For instance, covering the anisotropic Au nanomaterials with polydopamine to synthesise Au nanoworms resulted in stability after seven cycles of laser irradiation, efficient antibacterial activity, and good biocompatibility.[67] Furthermore, various species of ligands can be anchored on the AuNPs surface for surface modification of AuNPs to improve the photothermal antibacterial treatment. For example, Hu *et al.* [68] coated the Au NPs with a pH-responsive mixed charged zwitterionic layer for a good dispersion in the biological environment (pH ~7.4), excellent adherence to negatively charged methicillin-resistant *S. aureus* bacteria surfaces (pH ~5.5), and increased PTT performance. Similarly, the pH-responsive surface charge transition activities functionalised the Au NRs using polymethacrylate with pendant carboxyl betaine groups.[69] The hydrophobic/hydrophobic functionalisation of Au NRs substantially improved the antimicrobial efficiency promoting membrane disintegration. Hydrophilic functionalised polyethylene glycol (PEG)-Au NRs and hydrophobic functionalised polystyrene (PS)-Au NRs showed efficient bactericidal effects on *S. aureus* and Propionibacterium acnes (P. acnes) strains: the viable bacterial count reduced from ≤85% to ≥99.99% after exposure to NIR.[70] Other attempts to functionalise Au NRs consisted in (1) conjugating Au NRs with poly(2-lactobionamidoethyl methacrylate) and poly(2-fucose ethyl methacrylate) to specifically block bacterial LecA and LecB lectins of *P. aeruginosa* who mediate biofilm formation.[71] *In vivo,* experiments showed a fast temperature increase up to 60 °C and the removal of most bacteria from the infected tissue. Protease (bromelain)-conjugated Au NRs were also used to achieve rapid biofilm thermal degradation and advanced removal of exotoxins and auto-induced peptides. Enhanced enzymatic activity of bromelain against Gram-positive and Gram-negative bacteria upon NIR laser irradiation was observed. It was regulated within 30–60°C by the laser power adjustment.[72] Peptide and neuropeptide functionalised the surface of Au NRs through electrostatic interactions for targeted methicillin-resistant *S.aureus* and *E. Coli* binding and higher bactericidal activity than unconjugated Au NRs.[73] The functionalised photothermal materials were also stable for up to four cycles of NIR laser irradiation.

Silver (Ag), like Au, exhibits strong plasmonic properties in the visible region, where biological tissues absorb. Merkl *et al.* [74] obtained Ag plasmonic fractal-like nanoaggregates with tuneable extinction from visible to NIR wavelengths. Using SiO_2 during the flame synthesis of the spherical Ag NPs a dielectric spacer was created between plasmonic Ag NPs to tune plasmonic coupling, prevent any potential dissolution of Ag, and inhibit nanostructures' sintering or restructuring. The resulting nanomaterial was incorporated into a polymer layer and used as photothermal coatings on medical devices. Continuous laser irradiation at 808 nm completely eradicated *E. coli* biofilms after 5 min and *S. aureus* after 10 min. Interestingly, as Ag dissolves in biological media and hyperthermia accelerates the process and consumes the photothermal agent during PTT, Ag NPs-embedded hydrogel releases Ag^{+}, acting as PTA for antimicrobial PTT under a NIR laser.[75] Thus, nanostructures with plasmonic properties should be engineeringly changed to absorb in the NIR regions and be used in wound healing.[76–78]

Copper (Cu) alone is highly oxidised. Therefore, nanoCu can act as a nanoenzyme[79] with high photothermal conversion efficiency as it undergoes Fenton-like reactions in a wide pH range.

Preprints (www.preprints.org) | NOT PEER-REVIEWED | Posted: 16 May 2023 doi:10.20944/preprints202305.1106.v1

Notably, the atomically dispersed Cu ensured the photothermal properties and significantly improved the catalytic performance of Cu single-atom sites/N doped porous carbon (Cu SASs/NPC), which showed 100% antibacterial efficiency against *E. coli* and *MRSA* through photothermal-catalytic antibacterial treatment.[80] Furthermore, Cu SASs/NPC demonstrated good photothermal stability due to the particular structural configuration.

Palladium (Pd), used for photothermal cancer therapy, exhibits good photothermal stability and high optical extinction coefficients useful in bacterial photothermolysis. Recently, biocompatible PdNPs prepared via Bacillus megaterium Y-4 and biologically reduced and ultrasonically treated [81] presented improved photothermal conversion and bacterial ablation at low doses through an improved absorption in the NIR region.

Bismuth (Bi)-based nanomaterials with a bandgap of less than 1.53 eV can absorb in the NIR range. Pristine Bi, Bi-based compound nanomaterials and composites also expressed antibacterial PTT and PDT capabilities,[82] thus having the potential to treat bacterial infections. However, Bi oxidizes during irradiation, so strategies must be implemented to prevent this phenomenon and increase the Bi biomedical applications.

Bimetallic plasmonics. The chemical stability of Ag can be improved by debasing with Au to expand overall functionality. **Ag /Au bimetallic NPs** were synthesized onto a jellyfish-based scaffold. This antibacterial material can actively and spontaneously reduce Ag and Au ions and form NPs directly on the nanofibers' surface due to Q-mucin glycoproteins' presence in nanofibers.[83] The heat generated by small plasmonic NPs is more significant than the heat from the bigger and scattered NPs. The resulting materials proved to have combined actions against bacterial biofilm: disrupt/remove bacterial colonies and mature biofilms and prevent their regrowth. Another way to preserve the stable shapes of Ag NPs is to frame them with a more stable metal. Zhang *et al.* [76] proposed another type of architecture of AuAg yolk−shell cubic nanoframes with the nanosphere as the core and the cubic nanoframe as the outer shell. The existence of a void between the core and the shell parts came with some advantages, such as multiple reflections of the incident light between the shell and the core parts and an extensive electromagnetic field interaction between these unconnected parts. The material depolarises the bacterial membrane and affects the membrane potential, and the NIR laser exposure further increases the initial effect. TEM images of exposed *MRSA* showed leakage of intracellular substances. **Pd-Cu nanoalloy,** in combination with amoxicilli and encapsulated in zeolitic imidazolate framework-8, formed a complex antimicrobial system.[84] The photothermal nanoalloy significantly stimulates drug release, has good biocompatibility and has a significant antibacterial effect on planktonic bacteria and their biofilms.

Metallic compounds-based PTAs

Metal sulfides, oxides, selenides, and carbides, with lower cost than noble metals, are also used as PTAs due to their large surface area and facile surface modification. The nanomaterials have high photothermal conversion efficiency provided by the large band gap.

Copper sulfide (CuS) NPs transform light to heat due to the d–d transition of Cu^{2+}, and the maximum absorption peak cannot be shifted by changing the particle morphology. In practice, an NIR laser at 980 nm is used because some Cu-based nanomaterials need a high-powered NIR laser at 808 nm. The antimicrobial performance of CuS nanosheets via synergistic photothermal and photodynamic mechanisms depends on sulfur vacancies (Vs) concentration.[85] In the case of CuS, the CuS nanosheets with the highest Vs concentration achieved bactericidal rates of 99.9% against *Bacillus subtilis* and *E. coli* bacteria under 808 nm laser irradiation. The photothermal conversion efficiency was 41.8%. Similar results were obtained for other defect-rich CuS [86]. Recently, Chan *et al.* proposed a multifunctional platform (HNTs@CuS@PDA-Lys) to treat bacterial infections by synergistic lysozyme (Lys)-photothermal therapy.[87] The complex platform includes halloysite nanotubes (HNT), a natural clay mineral decorated with CuS, and a polydopamine (PDA) coating functionalised with antimicrobial enzyme Lys. HNTs@CuS@PDA-Lys exhibited excellent bactericidal activity against *E. coli* (100.0 ± 0.2 %) and *S. aureus* (99.9 ± 0.1 %), eliminating 75.9 ± 2.0 % of *S. aureus* biofilm under NIR irradiation (808 nm, 1.5 W/cm^2). Under NIR light exposure, a synthesised heterojunction composite of graphdiyne nanowalls wrapped hollow copper sulfide nanocubes

Preprints (www.preprints.org) | NOT PEER-REVIEWED | Posted: 16 May 2023 doi:10.20944/preprints202305.1106.v1

(CuS@GDY) also presented strong localised surface plasmonic resonance and enzyme mimic function.[79] The nanocomposite acts through the combined hyperthermic and increased peroxidase-like activities, facilitated by the exclusive hierarchical configuration, the tight bandgap of GDY nanowalls, LSPR effect of CuS nanocages, fast interfacial electron transfer dynamics, and carbon Vs on CuS@GDY. Also, Cu_7S_4-2 with (224) facets showed outstanding antibacterial efficiency against *B. subtilis*, *E. coli* and drug-resistant *P. aeruginosa* compared with Cu_7S_4-1 with (304) exposed facets via synergetic PDT and PTT.[86]

Molybdenum disulfide (MoS_2) belongs to the category of two-dimensional transition metal dichalcogenide nanosheets. Recently, its electronic structure was modulated by Vs engineering, with different concentrations of sulfur vacancies (Vs) being generated to optimize photothermal conversion efficiency. This strategy improves light absorption and avoids the recombination of photogenerated electrons-hols pairs. MoS_2 with abundant vacancy strongly binds to bacteria inhibiting colony formation. Above a specific concentration, excessive Vs on the surface of MoS_2 can be responsible for charge carriers blocking and photothermal performance decrease.[88,89] The photothermal conversion efficiency (η) was 45.97%, and bacteria were eliminated under the 808 nm NIR light irradiation. In another study, MoS_2 nanosheets were doped with copper ions (MoS_2@Cu2+) for reduced electron–hole recombination and improved photothermal efficiency.[90]

A biodegradable multifunctional **nickel sulfide** (NiS_2) nanozymes with photothermal performance, nano-catalysis property, and glutathione (GSH)- depleting function was proposed in [91]. This nanomaterial showed very good photothermal performance, catalytic properties, good stability, and rapid metabolism, proving a peroxidase-like ability to kill bacteria.

Biogenic **copper selenide** NPs (bio-CuSe) were incorporated in a polyvinylidene fluoride membrane to improve its qualities and antimicrobial properties. [92] NIR irradiation increased water temperature near the membrane, allowing for > 95% suppression of bacterial growth. The obtained conversion efficiency was 30.8%.

Tin selenides (SnSe) with different morphologies (sphere, rod, plate, and surface wrinkled) were investigated as PTAs. Spherical SnSe showed the best antimicrobial performance through combined photothermal and photodynamic mechanisms that managed to eliminate 99.99% of *E. coli* and *B. subtilis* bacteria.[93] The best calculated photothermal conversion efficiency was 41.4%, higher than other published values.

Ferrous-ferric oxide (Fe_3O_4) NPs have a strong enzyme-like catalytic ability in a wide pH range and can be used in a photothermal-enzymes combined antibacterial treatment platform. The photothermal effect can increase production of •OH from H_2O_2 through the Fenton reaction. Interestingly, the catalytic activity of Fe_3O_4 NPs intensifies with increasing temperature in the range of 25–50°C.[94] *In vitro* wound treatment with NIR laser after adding H_2O_2 damaged the biofilm. Also, the combined treatments showed less wound inflammation after in *vivo* tests. Lv *et al.* synthesised magneto-plasmonic multi-branched Fe_3O_4@Au core@shell nanocomposites [95] with a photothermal conversion efficiency of 69.9%, a complete bacteria ablation after NIR irradiation, good photo-stability and several times repeated use.

MXene materials, bidimensional transitional metal carbide/nitride, have gained increased attention since their discovery in 2011.[52] MXenes exhibit hydrophilicity and outstanding photothermal-conversion efficiency, which can lead to good antimicrobial activity.[96] Very recently, MXene were tested for antimicrobial applications and the results were unsatisfactory due to poor MXene-bacteria interactions and bacterial rebound *in vivo*. Ti_3C_2MXene was then used in a photothermal treatment and proved to have a unique membrane-disruption effect, with sharp edges of nanosheets acting as "nanoknives".[97] Different strategies were tried to improve antimicrobial efficiency. In [98], lysozyme was immobilized on titanium carbide Ti_3C_2TX MXene ultra-thin nanosheets modified with polydopamine for light-enhanced enzymatic inactivation of antibiotic-resistance bacteria due to close contact between this antimicrobial material and bacteria. In another study, Ti_3C_2TX MXene were combined with ciprofloxacin and incorporated in a hydrogel to trap and kill all the tested bacteria effectively.[99] An engineered interface between n-type Bi_2S_3 nanorods and Ti_3C_2Tx nanosheets produced more ROS due to the accelerated photogenerated charge separation

Preprints (www.preprints.org) | NOT PEER-REVIEWED | Posted: 16 May 2023 doi:10.20944/preprints202305.1106.v1

and transfer due to the differences between their work function values. Bi_2S_3 NR grew directly on the surface of Ti_3C_2Tx nanosheets leading to the generation of a potential contact difference and an increase in the local electron density on Ti_3C_2Tx, reducing the recombination of the electron-hole pairs. This nanocomposite was a stable, biocompatible, highly effective antimicrobial with enhanced photocatalytic and photothermal properties.[100]

Other inorganic PTAs

Black phosphorus (BP) is a layered two-dimensional (2D) semiconductor material applied as a photothermal agent due to its high photothermal conversion efficiency, extinction coefficient, biocompatibility, and excellent biodegradability.[101] BP exhibits less cytotoxicity than graphene, still being more toxic compared to other 2D nanomaterials.[102] Even without NIR irradiation, BP nanosheets can cause physical damage to the bacterial membrane, RNA leakage, and death because of the sharp edges of the sheets.[103] As a disadvantage, BP nanosheets can undergo rapid oxidation and degradation in ambient environments.[104] The photothermal conversion efficiency of BP nanosheets can be further enhanced by conjugation with Au. This nanocomposite can destroy up to 58% of Enterococcus faecalis bacteria from the biofilm under NIR light irradiation.[105] BP nanosheets decorated with cationic carbon dots (CDs) acted against bacteria through photothermal, photodynamic therapy, and electrostatic interactions between cationic CDs and bacteria walls.[106] CuS NPs were immobilized onto BP nanosheets resulting in an efficient synergistic nanocomposite for fighting *P. aeruginosa* and *S. aureus* cells.[107] After a few minutes of NIR irradiation, the temperature rises by 30.4 ◦C due to the photothermal conversion efficiency of both CuS and BP nanosheets. Recently, Zhao *et al.* [108] fabricated antibacterial photothermal nanofibres composed of polycaprolactone (PCL), Ag NPs and BP for infected wound healing. After irradiation, a significant increase in temperature was registered up to 41°C generated by the BP, and this hyperthermia accelerates the movement of Ag^+, avoiding the formation of silver aggregates. The *in vivo* studies indicated that the application of these complex nanofibres accelerated wound healing. Other studies proposed the conjugation of the two nanomaterials - BP and Ag NPs - in a BP@AgNPs nanohybrids with broadened visible light absorption [77] or a BP/Ag NPs nanocomposite [109] with higher efficiency for Gram-positive bacteria than Gram-negative bacteria.

Amorphous **red phosphorus** (RP) has rarely been applied despite its good biocompatibility. In one study, RP was used in a layered composite (with a graphene oxide layer on top), showing rapid and almost complete microbial inactivation under visible and NIR light.[110]

Boron. A multifunctional nanoplatform based on boron nanosheet (B NS)-coated quaternized chitosan (QCS) and the nitric oxide (NO) donor N,N′-di-sec-butyl-N,N′-dinitroso-1,4-phenylenediamine (BNN6). The B-QCS–BNN6 nanoplatform [111] exhibited photothermal therapy efficacy and provided controlled NO release after 808 nm laser irradiation, reaching fast >99.9% inactivation of bacteria.

Table 1. Representative new inorganic-based PTAs nanomaterials for antibacterial activity.

	Type of nanomaterials	Characterisation Morphology	Tested bacteria	PTT parameters	Performance	Ref.
Metalic based PTAs	Au NR	10 × 45 nm Au NR attached to glass surfaces	*S. epidermidis* ATCC 35984	LED - 850 nm, I=0.2 W·cm^{-2}, 5 min	AR=71% of biofilm Max- 97%	[61]
	Au nanaworms covered with PDA	Nanoworms with diameters of 5 ± 1.5 nm, interconnected	*E. coli* *S. aureus*	808 nm I=1 W·cm^{-2}, 20 min 100 μg·mL^{-1} PTAs	ΔT= 30.9 °C AR=80% *E. coli* and AR=90% *S. aureus*	[67]
	glycomimetic polymers decorated Au NR	AuNR- 50–100 nm long	drug-resistant *P. aeruginosa*	808 nm laser, I=2 W·cm^{-2}, 5 min 125 μg·mL^{-1} PTAs	ΔT= 15.4 °C AR=80%	[71]

Preprints (www.preprints.org) | NOT PEER-REVIEWED | Posted: 16 May 2023 doi:10.20944/preprints202305.1106.v1

	Protease (bromelain) - conjugated AuNR	Au NR -32 nm length, 7.8 nm width	*E. coli* *S. aureus*	808 nm 50 μg·mL^{-1} PTAs	T_{max} = 66°C AR=96.8% *E. coli* AR=97.9% *S. aureus*	[72]
	Peptides/neuropeptide conjugated AuNR	Au NR - 49 nm length and 11 nm width	*MRSA* *E. coli*	808 nm I= 2 W·cm^{-2}, 4 min	T_{max} ~70 °C stable after 4 cycles AR= 99% for *MRSA* AR= 96% for *E. coli*	[73]
	AuAg yolk−shell cubic nanoframes	well-defined cubic nanoframes 10 nm Au core and frame edge length: 25- 60 nm; frame thickness: 3.8 - 6.1 nm Ag/Au ≈ 3:1,	*MRSA* *E. faecalis* *P. aeruginosa* *K. pneumoniae* *B. bacillus* *E. coli*	808 nm laser I=0.33 W·cm^{-2}, 10 min	η = 65.6% at 0.27 W·cm^{-2} ‘; ΔT = 23.7 °C AR=96.55%, *P. aeruginosa* AR=93.69% *K. pneumoniae* AR=92.34 % *B. bacillus* AR=96.73%, *E. coli* AR=98.08% *E. faecalis*	[76]
	fractal-like Ag nanoaggregates in SiO_2 deposited on PDMS layer	AgNPs 10-20 nm, few nm interNPs distances SiO_2 =1.3-25%	*S. aureus and E. coli*	808 nm laser I=1.4 W·cm^{-2}, 10 min; m=15.4 μg Ag/SiO_2	η = 50% AR=100% of *S. aureus* biofilm (10 min) AR=100% of *E. coli* biofilm (5 min.)	[74]
	Pd NPs	4 nm and 41 nm in diameter	*S. aureus* and *E. coli.*	808 nm laser , I= 1.35 W·cm^{-2}, 10 min, 20 mg·L^{-1} PTAs	η = 33.1% AR=99.99% *S. aureus* AR=99.99% *E.coli.*	[81]
	Ag /Au bimetallic NPs on Jellyfish Nanofibers scaffold	Bimetallic Ag/AuNPs: nanospheres, nanotriangles	*B. subtilis* *P. aeruginosa* *E. coli*, S. epidermidis	808 nm NIR laser, I= 1 W·cm^{-2}, 5 min	T_{max}= 80 °C. Effective (AR=n.a.)	[83]
	Pd-Cu nanoalloy NPs+ AMO in ZIF-8	Spherical Pd-Cu nanoalloy NPs size 9.02 nm	*S. aureus* *P. aeruginosa*	λ = 808 nm NIR laser, I = 1 W·cm^{-2}, 10 min, 200 μg·mL^{-1} PTAs	η = 45.8% AR=99.8% *S. aureus* AR=99.1% *P.aeruginosa* CR= 75.3% *S. aureus* CR= 74.8% *P. aeruginosa*	[84]
Sulfid	Cu_7S_4 nanosheets	Cu_7S_4 samples with (224) exposed facet,	*B. subtilis*, *E. coli*	808 nm laser,	η = 40.52% ΔT= 29.4 °C	[88]

Preprints (www.preprints.org) | NOT PEER-REVIEWED | Posted: 16 May 2023 doi:10.20944/preprints202305.1106.v1

		a large number of nanosheets, diameter of 30–50 nm.	drug-resistant *P. aeruginosa*	I= 1.5 $W\cdot cm^{-2}$, 10 min, 50 $\mu g\cdot mL^{-1}$ PTAs	AR= 100% *E. coli* AR= 100% *B. Subtilis* , AR> 90% *P. aeruginosa*	
	CuS@GDY	graphdiyne nanowalls wrapped hollow CuS nanocubes	*MRSA* and *E.coli*	808-nm laser, I=0.4 $W\cdot cm^{-2}$, 10 min	η = 48%, ΔT= 28 °C AR >99.999% *MRSA* AR >99.999% *E.coli*	[79]
	CuS nanosheets with sulfur vacancies	Nanosheets: Diameters= 60–100 nm the thickness =25–30 nm	*B. subtilis* and *E. coli*	808 nm laser, I=1.2 $W\cdot cm^{-2}$, 10 min 50 $\mu g\cdot mL^{-1}$ PTAs	η = 41.8%, ΔT= 30 °C, AR=99.999% (both)	[85]
	sulfur vacancy modulated MoS_2	Nano spheres-diameter 200–300 nm	*E. coli*.	808 nm laser, I=1.5 $W\cdot cm^{-2}$; 10 min 50 $\mu g\cdot mL^{-1}$ PTAs	η = 45.97% ΔT 32 °C ≈100% killed bacteria	[89]
	Cu doped MoS_2 nanoflowers	Nanospheres of 50-500 nm; Cu^{2+} were uniformly distributed on the surface edge sites	*S. aureus*	660 nm laser, I=0.898 $W\cdot cm^{-2}$, 20 min., 2 $\mu g\cdot mL^{-1}$ PTAs	ΔT= 30.3 °C AR=99.64%	[90]
	NiS_2 nanozymes	Spherical NPs-diameter of 112 nm	*E. coli*, DH5α *MRSA*,Mu50	808 nm laser, I=0.75 $W\cdot cm^{-2}$, 10min, 75 $\mu g\cdot mL^{-1}$ PTAs	η = 43.8% ΔT= 23.4 °C AR=E.coli 98.33% AR≈92% MRSA	[91]
selenides	SnSe	spherical particles	*E. coli* and *B. subtilis*	808 nm laser, I=1.5 $W\cdot cm^{-2}$, 10 min 25 $\mu g\cdot mL^{-1}$ PTAs	η =41.4% Tmax =57 °C AR=99.99% *E. coli* and AR=99.99% *B. subtilis*	[93]
	Cu_2Se NPs in PVDF membrane	80 nm size NPs	*E. coli* and	1064 nm laser, I= 2.0 $W\cdot cm^{-2}$, 400 s 160 $\mu g\cdot mL^{-1}$ PTAs	η =30.8% ΔT= 14.6 °C AR=97.52% *E. coli*	[92]
Oxides	Fe_3O_4 NPs	mesoporous hollow Fe_3O_4 NPs	*E. coli* *S. aureus*	808-nm NIR + H_2O_2 (1mM) I=1 $W\cdot cm^{-2}$,10 min; 4 cycles 1 $mg\cdot mL^{-1}$ PTAs	η =28.5% AR=72% *S. aureus* and AR=100% *E. coli*	[94]

	magneto-plasmonic Fe_3O_4@Au core@shell	spherical core of Fe 3O4 and Au - branched structure	*E. coli* *S. aureus*	980 nm laser diode, I=1.0 W·cm^{-2}, 10 min, 50 µg·mL^{-1} PTAs	η = 69.9% AR=100% *E. coli* and AR=100% *S. aureus*	[95]
MXene	Ti_3C_2 MXene combined with Cip	Ti_3C_2 nanosheets monolayer with 50–200 nm lateral size	*E. coli* *MRSA*	808 nm, I=0.4 W·cm^{-2} , 15 min, 100 µg/mL Ti3C2+ 5 mg/mL Cip	Tmax =60.7 °C AR= > 99.99999%	[99]
	Ti_3C_2TX MXene-PDA functionalized +lysozyme	Ti_3C_2 MXene - monolayer	*MRSA*	808 nm laser, I=2.0 W·cm^{-2}, 15 min. 50 µg·mL^{-1} PTAs	η = 46.88% Tmax =63.5 °C. AR>95 % MRSA	[98]
	Bi_2S_3NR/Ti_3C_2Tx MXene	Ti_3C_2Tx Mxene few-layer nanosheets	*E. coli* *S. aureus*	808 nm light, I= 0.7 W·cm^{-2} , 10 min	η = 35.43% T_{max} =65 °C RA=99.86% *S. aureus* RA=99.92% *E. coli*	[100]
Other	BPs@cationicCDs	few-layer or monolayer BPs with a flat structure CDs (8–13 nm) grew in situ by BPs	*E. coli* *S. aureus*	660 nm + 808 nm laser, I=1.5 W·cm^{-2}, 5 min , 200 µg·mL^{-1} PTAs	η = 34.1% ΔT= 28.2 °C RA≈99 % *S. aureus* and *E. coli*	[106]
	BPQDs@NH	BP quantum dots (BPQDs) of 3 nm encapsulated in hydrogel	*MRSA* Amp^{r} *E. coli*	808 nm laser, I = 1 W·cm^{-2}, 5 min, 200 µg·mL^{-1} PTAs	η = 42.9% ΔT= 35 °C RA= 90% *MRSA* RA= 90% Amp^{r} *E. coli*	[112]

[1] ***Abbreviations***: PDA - polydopamine ; η - photothermal conversion efficiency; I - laser power densities (irradiance); Antibacterial rate- AR ; CR - clearance rate of biofilm; S. epidermidis - Staphylococcus epidermidis; MRSA - Methicillin-resistant Staphylococcus aureus; E. coli - Escherichia coli; B. subtilis-Bacillus subtilis; E. faecalis - Enterococcus faecalis; B. bacillus - Bauman bacillus; K. pneumoniae - Klebsiella pneumoniae; P. aeruginosa - Pseudomonas aeruginosa; PDMS - poly(dimethylsiloxane); PVDF- polyvinylidene fluoride; GDY- graphdiyne; Cip - ciprofloxacin ; ZIF 8 - zeolitic imidazolate framework-8; AMO - amoxicillin; QD - carbon dots.

Carbon-based nanomaterials

Carbon-based nanomaterials have attracted considerable attention as photothermal agents (PTAs) for antimicrobial applications, owing to their distinctive structure and outstanding optical, thermal/electronic, and mechanical properties, versatility in functionalisation, and high surface area [113], deep tissue penetration, and reduces mammalian cytotoxicity.[114]

Currently, from the entire carbon-based nanomaterials library, graphene-based nanomaterials (GBNs) and carbon nanotubes (CNTs) have become the hot spots to eradicate and deactivate bacteria *via* various physical and chemical antibacterial mechanisms such as chemical oxidation and ROS generation, biological isolation of microbial cells, generation of structural damages,[49] as well as photothermal effects [115,116], mainly being investigated as antimicrobial PTAs. The antibacterial properties of GBNs appear to be influenced by the presence and number of functionalities from their surface.[116] At the same time, CNTs are characterized by a size-dependent antibacterial activity that increases with a decrease in size.[117] Green fluorescent commercial graphene quantum dots (GQD) were tested as a photoactive antimicrobial agent, and a heat yield of 50% (measured by the photothermal lens technique) was obtained under excitation at 532 nm (wavelength shorter than the emission band), proving the potential to be an efficient, safe, and low-cost photothermal agent.[118] Carbon dots have also been tested due to their biocompatibility and versatility. One study reports the utilisation of bacteria-affinitive carbon dots targeting the D-Glutamic acid-adding enzyme (MurD ligase), which is involved in bacterial cell wall peptidoglycan synthesis.[119] Bacterial testing showed the ability of this material to kill 80.33% of *E. coli* and 89.27% of *S. aureus* without NIR light and, only after a few minutes of laser irradiation, more than 96% of *E. coli* and 100% *S. aureus* were killed, proving an increased spatial accuracy of the antibacterial action with minimal cytotoxicity to human cell lines.

In fact, as PTAs for antimicrobial applications, the carbon-based nanomaterials are usually combined with various compounds to improve the antibacterial performances through synergistic or additive effects, since their intrinsic photothermal properties, in some cases, cannot be sufficient to assure an appropriate antibacterial effect in a particular application. Thus, a great variety of reasonable **carbon-based combinations** with photothermal components (e.g., Au nanostars [120], fluorophores [121]) and antibacterial compounds (i.e. Ag NPs [122,123] have been designed and reported in the literature as efficient PTAs with adequate antibacterial activity in various practical applications (Table 2). For instance, Oruc *et al.* [121] decorated the surface of multiwalled carbon nanotubes (MWNT) with NIR-absorbing 3,3′-diethylthiatricarbocyanine (DTTC) fluorophores to obtain efficient photothermal nanomaterials that can kill *Pseudomonas aeruginosa*. Under NIR irradiation, the formulated MWNT/DTTC nanohybrids could produce a poweful hyperthermal effect (the temperature of the dispersion reached around 92°C after 15 min), leading to a 77% killing efficiency of *P. aeruginosa* cells. Then, the MWNT/DTTC nanohybrids were embedded within a waterborne polyurethane matrix. It was noted that under laser irradiation, the temperature increased to 120 °C, generating a substantial antibacterial and antibiofilm effect on *P. aeruginosa* cells attached to the surface. Further, Tan *et al.* [122] combined the excellent photothermal effect of RGO and intrinsic antibacterial features of AgNPs into RGO/Ag nanocomposite to destroy both common bacteria (*E. coli*) and multidrug-resistant (MDR) bacteria (*Klebsiella pneumoniae*). Among the investigated samples, RGO/Ag nanocomposite presented a significantly higher antibacterial activity against both bacteria, which synergistically increased under NIR irradiation (0.30 W/cm^2 for 10 min) through the photothermal effect that induced the cell membrane disruption and generation of ROS. In another work, Yang *et al.* [124] explored the synergy of photocatalytic-photothermal effects embedded in a stable BiOI-GO nanocomposite with better environmental disinfection properties, while Lv *et al.* [125] combined polyvinylpyrrolidone-functionalized AgNPs with rGO (AgNPs-PVP@rGO) into a visible-light-triggered photoactive nanocomposite able to increase the visible-light-driven photocatalytic degradation and photothermal antibacterial activity.

Albeit carbon-based nanomaterials are characterized by a series of advantages, such as profuse source, low cost, thermal and mechanical stability, good processability, and high thermal conductivity, besides biocompatibility issues, the relatively low photothermal effect for antibacterial activity represents the main drawback as PTAs, particularly when compared to photothermal effect generated by the inorganic or noble metals-based nanomaterials.

3.2. Organic based PTAs

Recently, organic compounds-based nanomaterials have received increasing attention as potential alternatives to inorganic-based nanomaterials, being extensively exploited in formulating PTAs with proper antibacterial activity. As PTAs, these compounds typically absorb photons produced by NIR irradiation and generate heat through non-radiative relaxation pathways. The category of organic-based PATs nanomaterials is generally represented by conjugated polymers-based nanomaterials (i.e., polyaniline, polypyrrole), crystalline porous organic polymers (e.g., covalent organic framework) and polymer functionalised nanomaterials.

Conjugated polymer (CP)-based nanomaterials

Among various classes of macromolecules, conjugated polymers (CP) with absorption in the NIR range, such as polydopamine (PDA), polyaniline (PANI), polypyrrole (PPy), or poly(3,4-

Preprints (www.preprints.org) | NOT PEER-REVIEWED | Posted: 16 May 2023 doi:10.20944/preprints202305.1106.v1

ethylenedioxythiophene) (PEDOT), are widely explored in designing new light-responsive nanomaterials with suitable antimicrobial and bactericidal performances. Besides the inherent electronic and optical features originating from the specific delocalised electronic structure and the presence of large π-conjugated backbones [117,126], CP is characterized by low light scattering and high penetration depth of NIR light in tissue, amenability in formulation, as well as higher biocompatibility than carbon-based nanomaterials, capable of mitigating their main drawback related to agglomeration.[126] To maximize the bacterial interaction capability, aqueous stability, and antimicrobial PT effect, CP is usually modified with different compounds (i.e. cationic ammonium groups, PEI, Au nanorods, Au NPs, magnetic NPs) (Table 2).[127] Zhou *et al.* [128] formulated positively charged conjugated polymer (PTDBD)-based NPs with NIR-triggered activity and better bacterial interaction ability for antimicrobial therapy to advance the phototherapy for bacterial infections,. Under a low power light density of 1 $W\cdot cm^{-2}$ (808 nm) and a short time of 8 min, simultaneous ROS and heat generated by the polymer PTDBD with donor-acceptor (D–A) structure could effectively kill three representative microbes (e.g., *Ampr E. coli*, *S. aureus*, and *C. albicans*. Further, the authors investigated the efficacy of this strategy *in vivo* for treating *S. aureus*-infected wounds of mice, noticing no significant damage to normal tissue, demonstrating its great potential in the application of treatment for bacterial infections. Later, Zhang *et al.* [84] used the same strategy to design cationic conjugated PDTPBT NPs for photothermal antibacterial therapy under NIR light irradiation. Based on the *in vitro* experiments, the constructed PDTPBT exhibited efficacious antibacterial ability upon 808 nm laser irradiation, besides excellent photostability and high photothermal conversion efficiency. In another work, Ko *et al.* [129] constructed a photothermal nanocomposite based on poly(3,4-ethylenedioxythiophene): poly(styrene-sulfonate) (PEDOT: PSS) and agarose with thermo-processability, light-triggered self-healing, and excellent antibacterial activity. The authors demonstrated that during NIR exposure, PEDOT: PSS/agarose exhibited high shape flexibility through the NIR light-induced self-healing effect after damage and excellent antibacterial activity against pathogenic bacteria, successfully destroying and killing *E. coli* and *S. aureus* within 2 min of irradiation.

Polymer functionalised nanomaterials

Functionalising nanomaterials with specific polymers (i.e. PEG, chitosan, peptides) is a widely exploited strategy that, besides improving biocompatibility, dispersibility, protection in the biological environment and specific targeting, may increase the physicochemical properties or endow the newly formulated nanomaterials with specific functions, advancing their effectiveness in PATs in practical antibacterial applications [130] (Table 2). In this respect, Fan *et al.* [131] managed to construct photothermal NPs that could efficiently kill *E. coli* at a relatively low temperature of ~45 °C under NIR irradiation by linking PDA NPs with thiolated poly-(ethylene glycol) (PEG) and magainin I (MagI) for increasing the stability and bacterial interaction specificity. Jia *et al.* [132] constructed a versatile graphene-based photothermal nanocomposite that could rapidly and effectively eliminate Gram-positive - *S. aureus* and Gram-negative - *E. coli* bacteria, supplementary destroying bacterial biofilms upon NIR irradiation. In this sense, the authors combined the efficient ability of chitosan to capture the bacteria by its positively charged functional groups with magnetic NPs and the photothermal conversion efficacy of GO. The formulated multifunctional nanocomposites could eliminate bacteria effectively after 10 min of NIR irradiation and destroy bacterial biofilms, suggesting their great potential in antibacterial applications. In another work aiming at resolving focal infection generated by antibiotic-resistant bacteria, Korupalli *et al.* [133] used the same strategy. They developed pH-responsive self-assembly into NPs based on polyaniline-conjugated glycol chitosan (PANI-GCS). The authors estimated that under NIR irradiation, the local temperature of PANI-GCS NPs increased by approximately 5°C leading to the specific and direct aggregation of bacteria, avoiding tissue damage, and promoting the wound healing. Furthermore, Wang *et al.* [134] proved that the functionalisation of photothermal-responsive conjugated polymer nanoparticles with cell-penetrating peptide (CPNs-Tat) might be considered a rapid and effective modality for combating bacterial infections. The positively charged Tat from the surface of NPs could efficiently enhance the interaction with bacteria cells leading to CPNs-Tat/bacteria aggregation. At the same

Preprints (www.preprints.org) | NOT PEER-REVIEWED | Posted: 16 May 2023 doi:10.20944/preprints202305.1106.v1

time, under NIR irradiation, CPNs-Tat could convert the light into heat efficiently and produce local hyperthermia to kill bacteria within a few minutes.

Covalent organic frameworks

Covalent organic frameworks (COFs) represent crystalline organic frameworks of porous polymers. Besides, good thermal stability, reduced toxicity, and versatility in functionalisation contain specific light atoms (carbon, nitrogen, oxygen, and borane), tailored and harmonious porosity.[135,136] These features enable them to be considered tremendous candidates for developing suitable platforms for application in different fields (i.e. gene and drug delivery, bioimaging, biosensing) [135], mainly being used as wound healing and antibacterial agents, owing to their long-lasting antibacterial properties and ability to interact with the bacterial cells through their hydrophobic spatial structures.[137] In addition, the encompassed light lightweight elements, strongly connected with covalent bonds along with specific 2D (two-dimensional) or 3D (three-dimensional) π-conjugation structure, make them critical light-activated agents for photothermal and photodynamic antibacterial effect, as well as in combinatorial therapies [135–138]. Porphyrin-based COF (TP-Por-CON) containing nitric oxide (NO) donor molecule, BNN6, within the pore volume of the framework structure for synergizing photodynamic, photothermal and gaseous therapies under red light irradiation (635 nm) and efficiently killing Gram-negative bacteria *E. coli* and Gram-positive bacteria *S. aureus in vitro* was successfully synthesized.[139] Yang *et al.* [140] reported the construction of a covalent organic framework (TAPP-BDP) with a conjugated donor-acceptor) structure. Under the NIR-irradiation (λ = 808 nm), it can exercise triple and synergistic bacterial inhibition by combining photodynamic, photothermal, and peroxidase-like enzymatic activities. Based on *in vitro* investigations, the authors proved the excellent antibacterial efficiency of TAPP-BDP against Gram-negative and Gram-positive bacteria. At the same time, the *in vivo* experiments further suggested the ability of materials to heal wounds infected with *S. aureus* in animals. Recently, Li *et al.* [136] have proposed a rational strategy for treating drug-resistant pathogenic bacterial infection by constructing a hydrogel with photocatalytic and anti-inflammatory activities based on Cu co-coordinated D- A type COF and sodium alginate hydrogel (CTCS) for adequate healing of wound infection. Under the NIR-irradiation (λ = 660 nm), the CTCS hydrogel presented an excellent bactericidal activity originated from the synergy of photothermal and photocatalytic effects, killing 99.95% and 98.5% of *S. aureus* and *E. coli* of bacterial strains within the first 20 min. *In vivo* experiments confirmed that CTCS hydrogel could be used as a strategy for rapid reconstruction of bacterially infected tissues, owing to their ability to reduce the expression of TNF-α and promote wound healing and tissue regeneration (IL-10 and VEGF).

Table 2. Representative C-based and organic-based PTAs nanomaterials for antibacterial activity.

	Matrix/ material	Light (nm) and power	Temperature reached	Antibacterial mechanism	In vitro biological performances		Ref
					Type of bacteria	*Efficacity*	
Carbon-based nanomaterials	rGO/AuNP	808 nm; 3.0 W/cm^2	73.5 °C	PTT	*S. aureus* *E. coli*	100%	[120]
	MWNT/DTTC	808 nm; 1.0 W/cm^2	92 °C, 120 °C	PTT	*P. aeruginosa*	77% -100%	[121]
	GO/Ag	808 nm; 1.5 W/cm^2	24.6 °C	PTT & Ag^+ release	*MDR E. coli*	~ 96%	[123]
	rGO/Ag	808 nm; 0.30 W/cm^2	Higher with ~ 20 °C	PTT &Ag^+ release	*E. coli,* *K. pneumonia*	100%	[122]

Preprints (www.preprints.org) | NOT PEER-REVIEWED | Posted: 16 May 2023 doi:10.20944/preprints202305.1106.v1

	AgNPs PVP@rGO	Visible-light	-	PTT & Ag^+ release & physical wall demolition	*E. coli*	Effective	[125]
	Fe_3O_4@GO-QCS	808 nm; 3.0 W/cm²	≥50 °C	Bacteria capture & PTT & Magnetic Recycle	*S. aureus* *E. coli*	~ 100%	[141]
	Fe_3O_4-CNT-PNIPAM	808 nm; 3.0 W/cm²	-	Bacteria capture & PTT & Magnetic Recycle	*S. aureus* *E. coli*	~ 100%	[142]
CP	PTDBD	808 nm; 1.0 W/cm²	66 °C	PTT	*S. aureus* *E. coli* *C. albicans*	Effective	[128]
	PDTPBT	808 nm; 1.0 W/cm²	57 °C	PTT	*E. coli* *MRSA*	Effective	[84]
	PEDOT:PSS/agarose	808 nm; 2.0 W/cm²	24.5 °C	PTT	*S. aureus* *E. coli*	~ 100%	[129]
	PDPP3T	808 nm; 0.50 W/cm²	~ 45°C	PTT	*E. coli*	~ 100%	[143]
	DMCPNs	808 nm; 0.50 W/cm²	62.4 °C	PTT & PDT	*E. coli*	93%	[144]
Polymer functionalized nanomaterials	MagI-PEG@PDA NPs	808 nm; 2.0 W/cm²	45 °C	PTT	*E. coli*	99.99%	[131]
	GO–IO–CS nanocomposite	808 nm; 2.0 W/cm²	~ 25°C	PTT & capture bacteria & aggregation	*S. aureus* *E. coli*	~ 80%	[132]
	CPNs-Tat	808 nm; 2.0 W/cm²	55.3 ºC	PTT	*E. coli* *S. aureus* *C. albicans*	~ 100%	[134]
	SF-CS-PDA cryogels	808 nm; 2.0 W/cm²	~ 45 °C	PTT & ROS-scavenging capacity, tissue affinity	*S. aureus* *E. coli*	Effective	[145]
COFs	TP-Por-CON@BNN6	635 nm	-	PTT & PDT & gaseous therapy	*S. aureus* *E. coli*	Effective	[139]
	TAPP-BDP	808 nm	65 °C	PTT & PDT & ROS	*S. aureus* *E. coli*	Effective	[140]

Preprints (www.preprints.org) | NOT PEER-REVIEWED | Posted: 16 May 2023 doi:10.20944/preprints202305.1106.v1

CTCS	660 nm 0.4 W/cm^2	~ 54 °C	PTT & PDT	*S. aureus* *E. coli*	> 98.5%	[136]

Abbreviations: AuNP - gold nanostar; MWNT - multiwalled carbon nanotubes; DTTC - 3,3′-diethylthiatricarbocyanine fluorophores; AgNPs PVP@rGO - polyvinylpyrrolidone-functionalized silver nanoparticles combined with reduced graphene oxide; GO-QCS - quaternized chitosan anchored graphene oxide; Fe_3O_4 -CNT-PNIPAM - poly(N-isopropylacrylamide) chemically grown onto the surface of carbon nanotube (CNT)– Fe_3O_4 ; PTDBD - positively charged conjugated polymer; PDTPBT - cationic water-soluble conjugated polymer based on a donor–acceptor (D–A) structure; PEDOT:PSS/agarose - Poly(3,4-ethylenedioxythiophene): poly (styrene-sulfonate)/agarose nanocomposite; PDPP3T - diketopyrrolopyrrole-based conjugated polymer; DMCPNs - dual-mode conjugated polymer nanoparticles based on poly(diketopyrrolopyrrole-thienothiophene) (PDPPTT) and poly[2-methoxy5-((2-ethylhexyl)oxy)-p-phenylenevinylene] (MEH-PPV); MagI-PEG@PDA NOPs - Magainin-modified polydopamine nanoparticles; GO–IO–CS - chitosan-iron oxide - functionalized magnetic graphene oxide; CPNs-Tat - photothermal-responsive conjugated polymer nanoparticles functionalized with cell-penetrating peptide; SF-CS-PDA – polydopamine nanoparticles incorporated into chitosan/silk fibroin cryogel; TP-Por-CON@BNN6 - Porphyrin-based covalent organic framework containing nitric oxide and BNN6; TAPP-BDP - covalent organic framework with a conjugated donor–acceptor (D–A) structure; CTCS - Cu co-coordinated D-A type COF and sodium alginate hydrogel.

Although the photothermal effect of organic-based nanomaterials usually does not outperform that of inorganic materials, these materials have attracted tremendous attention as PTAs, owing to biocompatibility and potential biodegradability, essential features that are missing in the case of inorganic materials, and which can be further fine-tuned depending on the targeted application.

Among investigated materials, CP and COFs are characterized by relatively good biocompatibility, significant absorption coefficient, and high photothermal conversion efficiency. In contrast, besides the acceptable biocompatibility, functionalised polymer nanomaterials, are endowed with specific targeting segments, which may resolve the most faced challenge of nanomaterials and the agglomeration process and increase the PTT performances as antibacterial.

Despite many optimistic outcomes of organic-based PTT, there are still practical barriers to clinical translation. First, their synthesis/formulation can be expensive and laborious, so simple preparation methods for scale-up are still needed. Second, in vitro and in vivo studies related to long-term biosafety are still in their infancy and are challenging. At the same time, the biodegradation mechanism of complex organic structures such as PTAs in living organisms still needs to be investigated. Therefore, further investigation is required to design more biocompatible organic-based PATs with predictable biodegradation mechanisms and biological behaviour that would satisfy PTT efficacy.

3.3. Hybrid photothermal antimicrobials and inorganic-organic nanocomposites

Metal-organic framework (MOF)-derived hybrid materials developed as promising multifunctional nanomaterials or nanocarriers for medical applications such as diagnosis and antimicrobial therapy. [146] Moreover, NPs can be incorporated into the hydrogels and used as nanocomposite hydrogels. The NPs can be added directly to the hydrogels, produced in situ via reaction within the hydrogels, or mixed with a hydrogel precursor to undergo gelation and form the final NPs hydrogel. Interestingly, the nanocomposites' high chemical or physical complexity allows synergistic effects and better functionality.[147] Therefore, hybrid nanosystems have been increasingly developed for their versatility and efficacy in overcoming obstacles not readily surmounted by nonhybridised counterparts.

For instance, rough surface nanoparticles with satisfactory biocompatibility, such as carbon-iron oxide nanohybrids with rough surfaces (RCF) [148] or $NiFe_2O_4$@Au/PDA[149] demonstrated antibacterial effects via synergistic photothermal therapy (PTT)/chemodynamic therapy (CDT) effects in the NIR-II bio-window and photothermal-magnetolytic, respectively. The nanostructures presented increased bacterial adhesion for effective interaction, better penetration depth and low

Preprints (www.preprints.org) | NOT PEER-REVIEWED | Posted: 16 May 2023 doi:10.20944/preprints202305.1106.v1

power density in vitro and *in vivo* studies against E. Coli, S. Aureus, and MRSA. Excellent antibacterial activity against S. aureus (99.7%) and P. aeruginosa (99.9%) occurred under heat-induced antimicrobial agent physcion（Phy）release from the drug-loaded black phosphorus nanosheets (BPNSs@phy).[150] The BPNSs presented excellent photothermal conversion ability, which disturbed the hydrophobic interactions that kept the antibiotic onto the nanosheets and facilitated Phy release, thus the PTT/CDT synergism for a better bactericidal effect.

Furthermore, loading hydrogels with nanoparticles increased their functionality. The fluorescent carbon dots (CDs) employed as carriers for curcumin (Cur) within the CDs/Cur Nanocomposite [151] exhibited low cytotoxicity and negligible haemolytic activity. IK8-liposome/AuNR-loaded hydrogels [152] incorporated antimicrobial peptides-loaded liposomes, IRIKIRIK-CONH$_2$(IK8) and gold nanorods (AuNRs) into poly(ethylene glycol) (PEG) to protect them from proteolysis and to employ the PTT capacity for a controllable PTT/CDT synergistically enhanced antibacterial nanoplatform against S. aureus and Pseudomonas aeruginosa.

Enhancing the antibacterial activity of silver ions (Ag+) was possible through a silver nanoparticle-embedded carrageenan hydrogel, the gallic acid-modified silver nanoparticles (GA-Ag NPs Carr)[90] and antimicrobial peptides-gold/silver nanorods (Dap@Au/Ag NRs)[153] capable of destroying the integrity of the MRSA membrane and resulting in content leakage and bacterial death. The platforms expressed PTT/CDT enhanced antibacterial activity via Ag+ released from the NPs and NRs, and NIR laser-induced photothermal assistance GA-Ag NPs and Au/Ag NRs. The hydrogels also presented good biocompatibility and effective anti-*S. aureus*, *MRSA* and *E. Coli* activity and healing-promoting properties *in vivo*. Similarly, wound healing was accelerated in diabetic rats when studying a black phosphorus quantum dots-based hydrogel (BPQDs@NH).[154] The MRSA-infected wounds exposed to the combined PDT/PTT were effectively sterilised due to the rapid increase in temperature (up to 55 °C), ROS production, lipid peroxidation, glutathione, adenosine triphosphate accumulation and bacterial membrane destruction. 99.64% efficacy against *Staphylococcus aureus resulted from the* enhanced photocatalytic and photothermal performances of Molybdenum disulfide (MoS_2) nanosheets doped with copper ions (MoS_2@Cu^{2+}).[90] The underlying MOA consists of the combined hyperthermia, ROS and Cu^{2+} release. The Cu^{2+}, by absorbing photons and converting the photoenergy into heat (the d–d transition of electrons), contribute to intense PTT. At the same time, the Cu^{2+} also absorbs the photogenerated electrons from MoS_2 and contributes to enhanced ROS (reducing electron-hole recombination). Despite the promising initial results, developing effective MoS_2-based antibacterial nanomaterials is still problematic due to the hydrophobicity and the weak interaction with bacteria and ROS. Therefore, constructing polyethylenimine modified Molybdenum disulfide (MoS2-PEI) nanocomposite enhanced the stability and promoted the binding to the surface of bacteria through electrostatic interactions for enhanced photothermal antibacterial activity [155] and even a combined chemo/photothermal/photodynamic triple-mode therapy of bacterial and biofilm infections. [156] Under NIR light irradiation, MoS_2-PEI exhibited evident synergistic antibacterial efficacy against *Escherichia coli* and *Staphylococcus aureus* with a long-term bactericidal effect. High-efficiency bactericidal and long-term bacteriostatic effects with less bacterial rebound were observed in an MRSA-induced murine abscess under PTT with Ti3C2MXene-based hybrid hydrogel. The rationally designed MXene-based hybrid hydrogels provided a strategy for cost-effectively treating localized bacterial infection by nanosystems.[99] Exploiting the photothermal sensitivity and peroxidase-like activity against one strain of vancomycin-intermediate S. aureus reference strain and E. coli proved successful due to the encapsulated tungsten sulfide quantum dots (WS_2QDs) and vancomycin (VAN) in thermal-sensitive liposomes. Interestingly, the enzymatic properties of WS_2QDs, the intrinsic and the temperature-dependent ones, contributed to the improved CDT efficacy, illustrating the platform's potential as one controllable system. The nanosystem also achieved antibiofilm properties via biofilms' disruption for better drugs' transmembrane passage. Moreover, the in vivo studies highlighted biocompatibility and the possibility of engaging the synergistic chemodynamic/photothermal antibacterial effects as reliable therapeutic approaches.[157] One complex nano-platform based on a hybrid structure was proposed as a novel therapeutic option for MRSA skin infections. In this case, the system incorporated two-

Preprints (www.preprints.org) | NOT PEER-REVIEWED | Posted: 16 May 2023 doi:10.20944/preprints202305.1106.v1

layered microneedle (MN) arrays: one water-insoluble inner layer with NIR photothermal capacity was encased by one water-soluble external layer loaded with vancomycin (VAN). The photothermal core comprised flame-made plasmonic Au/SiO_2 nanoaggregates and polymethylmethacrylate (PMMA). The evaluation showed a synergistic CDT/PTT (VAN and heat above 55 °C for 10 min) effect, which reduced the methicillin-resistant *Staphylococcus aureus* (MRSA) survival by up to 80%.[158] The antibacterial and wound-healing capacity of injectable and self-healing hybrid hydrogels showed high-efficiency photothermal antisepsis under mild PTT conditions. The hybrid hydrogel prepared by self-polymerising dopamine into polydopamine and synchronised reduction of Ag^+ to Ag NPs within a chitosan scaffold presented spontaneous recovery after mechanical damages, maintained the structural integrity, and recovered the original admirable antimicrobial functions *in vitro* and *in vivo* with no obvious toxicity.[159] Since the toxicity of certain nanocomposites such as AuNPs needs to be mitigated prior to incorporating them into nanoplatforms for biological use, one strategy was proposed: having the AuNPs immobilized onto a larger particulate system, a natural clay halloysite nanotubes (HNTs) and the HNTs modified with antibodies against *Escherichia coli* (*E. coli*, as a model microorganism) for immune-targeted PTT. The resulting AuNR-Ab-HNTs hybrids demonstrated that the harnessing antibody-functionalized HNTs as carriers increase the potential of the functionalised PTT/immunotherapy nanoplatforms for targeted delivery of antibacterial nanoparticles combinations (e.g., silver or metal oxides) or antibiotics for the localized antimicrobial infections.[160]

In conclusion, the advances in nano-biotechnology are promising and pave the way towards NIR-controlled multimodal potent antibacterial hybrid platforms without apparent toxicity. Designing and manufacturing intelligent nanosystems as more effective and selective alternatives will address the worldwide expansion of antibiotic-resistant species and the need to protect the microflora from non-specific antibiotics.

4. Applications

There are many expectations PTAs must meet to comply with the essential criteria for future clinical implementation. There are vital technological and pharmacological requirements, from finding the suitable nanomaterials and incorporating them into easy-to-manufacture devices to the efficacy, efficiency and biosafety to cost-effectiveness and user-friendliness. In the case of potential applications, the examples that follow also explain the need for standardisation despite the difficulties in managing the wide variety of nanomaterials used in various conditions of concentration,[120] power densities, wavelength, laser light's power, exposure time and focal spot size,[72,73] the type of bacteria, the antibacterial MOA for the best efficacy and highest safety to the tissues.[6,8,11,18–20] The ideal will be intelligent nanosystems to respond to the microenvironment and deliver safely.

4.1. Anti-bacterial biofilms

Biofilms are 3D complex structured grouped bacteria adherent to a surface and embedded in an autogenerated matrix of extracellular polymeric substances. The biofilm matrix comprises various extracellular polymeric substances (EPS), such as polysaccharides, proteins, amyloids, lipids and extracellular DNA (eDNA), membrane vesicles and humic-like microbially derived refractory substances.[161] Biofilms enhance antimicrobial resistance via mechanisms yet to be elucidated,[162] thus nanoparticles' anti-biofilm capacity depends on many factors, such as biofilm maturity, surface composition and chemistry, nanoparticle size, surface charge, surface chemistry, and nanoparticle concentration [163]. Generally, anti-biofilm nanomaterials either destroy the biofilm or interfere with the biofilm formation. Interfering with biofilm formation [154] could be one method to address bacterial infections and wound healing.[164] Moreover, penetrating the almost 50 μm thick infectious biofilms [21] requires transporting the antimicrobials through hydrophilic biofilm channels [22–24] and no absorption into the channels' walls.[25] Also, nano-antimicrobials should resist reticuloendothelial rejection during transport within the vascular system, [26,27] which limits their operative size to between 100 – 200 nm.[28] Therefore, the ideal PTT-based antibacterial and anti-

Preprints (www.preprints.org) | NOT PEER-REVIEWED | Posted: 16 May 2023 doi:10.20944/preprints202305.1106.v1

inflammatory photothermal agents (PTAs) should present high photothermal conversion efficiency and stability, good biosafety, responsivity to the microenvironment [165] and cost-efficient fabrication[166] via the right combinations of antimicrobial mechanisms [167,168] and patient-friendly devices.[169]

The experiments *in vitro* and *in vivo* specified the success rates and challenges of PTAs as anti-biofilms. BSA@MPN + NIR treatment induced long-term varying degrees of bacterial membrane malformations and achieved >99 % eradication of biofilms of *S. aureus* and *E. coli.*[170] Meanwhile, graphene and its derivatives, graphene oxide (GO) and reduced GO (rGO), due to their intrinsic properties and functionalisation with metal NPs, natural compounds, and antibiotics, could damage the bacterial morphology and release intracellular substances and destroy the biofilm. The agglomerated structure of GO hydrogels (i.e., chitosan, collagen, or polyvinyl alcohol) could entrap and stack the bacteria, preventing their initial attachment and biofilm formation. The sharp edges of GO could destroy the extracellular polymeric substance surrounding the biofilm and ruin the biofilm biomass structure.[171] Ag+ released from the Ag NPs in Ag NPs-incorporated quaternized chitin (DQCA) nanomicelles[78] interacts with proteins and enzymes and significantly deforms the bacterial membrane structures. At the same time, the high concentrations of ROS produced perturb cellular metabolism.[172,173] (Ag+-GCS-PDA@GNRs) [174] faster releases Ag^+ in a pH-controlled manner to increase the bacteria membrane permeability, pierce them even at a very low dosage, and thermally damage the membranes of Gram (+) and Gram (-) bacteria. Interestingly, the local hyperthermia increases the Ag+ release concurrently and further improves the nanoplatform's chemotherapy effect via a synergistic antibacterial mechanism. Unfortunately, despite the superior antibacterial properties of Ag NPs, the high cost and toxicity to humans (i.e. argyria, muscle spasms, gastrointestinal disorders) limited the larger *in vivo* applications.[175,176] Upon NIR irradiation, nanocomposites with a gold core and copper (I, II) sulfide shell ($Au@Cu_{2-x}S$) were shown to destroy *Enterococcus faecalis* and *Fusobacterium nucleus* biofilms through the decomposition of microbial exopolysaccharides during photothermal and peroxidase-like catalytic activity. [177] Interestingly, a low exogenous (NO) concentration can enter bacteria and provide a degree of antimicrobial activity through physical and functional changes. [178] NO activation and local less intense hyperthermia (<45^{o}C) represented the primary mechanism of effective biofilm elimination *in vivo*. Importantly, AI-MPDA acted as an all-in-one cytocompatible platform via the NO-enhanced PDT, while the low-temperature PTT that severely disrupted the bacterial membranes prevented bacterial colonisation.[179] In Cip-Ti_3C_2 TSG, the ''nano knives'' and PTT that led to the membrane damage could improve the penetration of Cip to achieve high-efficiency sterilisation. In addition, the functionalized Ti_3C_2 nanocomposites with cationic Cip can combine with the bacteria membrane through electrostatic interaction, which was conducive to the capture and killing of MRSA.[99] Among the new strategies using dissolvable microneedle (MNs) patches proved potential. The a-amylase-PDA@Levo microneedles, fabricated via a two-casting method, incorporated levofloxacin dopamine NPs (PDA@levo), a-amylase as the active ingredients and Polyvinyl alcohol (PVA) as the fast dissolution matrix. Under NIR, the MNs effectively delivered the enzymes, antibiotics, and PTAs into the cellular membranes. Enzymolysis destroyed the structure of the EPS matrix (extracellular polysaccharides) to eradicate biofilms, while PDA@Levo nanoparticles eradicated biofilms and killed the exposed bacteria via synergistic chemotherapy - PTT. The entire process also reduced inflammation time and promoted wound healing and tissue regeneration.[180]

As mentioned, interfering with bacterial physiological functions is also one possible MOA of the NIR-activatable anti-biofilm activity of PTAs. One study explains how Deoxyribonuclease (DNase)-carbon monoxide (CO)@mesoporous polydopamine nanoparticles (MPDA NPs) efficiently eliminated MRSA biofilm through DNA degradation and microbial destruction by CO gas molecules.[181] A titanium implant was covered with black phosphorus and a complex hydrogel formed by poly(vinyl alcohol) modified with chitosan, polydopamine, and a nitric oxide release donor to eradicate MRSA biofilm and to support osteogenesis. NIR light irradiation generated peroxynitrite ($\bullet ONOO^-$)that impacted the gene regulation of biofilm formation factors (intercellular adhesion gene D-icaD; intercellular adhesion gene A-icaA, staphylococcal accessory regulator -SarA),

Preprints (www.preprints.org) | NOT PEER-REVIEWED | Posted: 16 May 2023 doi:10.20944/preprints202305.1106.v1

as well as virulence factors (α-hemolysis, staphylococcal enterotoxin A) halting MRSA biofilm formation.[182] Protease-Conjugated AuNR antibacterial system reduced surviving bacterial populations to 3.2% and 2.1% of untreated control numbers for *E. coli* and S. aureus, respectively, and inhibited biofilm formation and exotoxin secretion even in the absence of NIR radiation. However, enhanced degradation of existing biofilm and exotoxin was observed when PGs were used with NIR laser irradiation. This promising new strategy achieved both the reduction of viable microorganisms and the elimination of biofilm and exotoxin. Thus, this strategy addresses the long-ignored issue of the persistence of bacterial residues that perpetuate chronic illness in patients even after viable bacteria have been eradicated.[72] Intriguingly, the enhanced protease stability due to immobilisation may protect the enzyme from inactivation would boost enzymatic degradation of bacterial surface transmembrane proteins or signal molecules (such as AIP) to further reduce bacterial viability, even at suboptimal temperatures. Moreover, according to previous studies, the photothermal effect, regarded as an internal heating model, could boost the activity of the conjugated enzymes, which may lead to a synergistic effect.[183]

Notably, functional coatings using immobilized photothermal agents are efficient means for sterilisation via breaking down and stopping biofilm formation. These compounds target Quorum sensing (QS) molecules and virulence factors and disturb the essential intercellular signalling mechanism, which regulates biofilm formation, virulence, formation of spores or fruiting bodies, apoptosis, and genetic competence.[184] Furthermore, the combined modalities proved efficient antibacterial potential through synergistic PTT, PDT and chemotherapy effects for inhibiting biofilm formation and killing deep biofilm bacterial cells.[156]

4.2. Synergistic photodynamic effects-based antibacterial systems

The PTT-induced hyperthermia on the healthy surrounding tissues, [185,186] the hypoxia in the deep infection microenvironment which reduces PTT efficiency [187,188], the excess ROS causing inflammation, fibrosis, and necrosis of normal cells [189] or the low catalytic activity of CDT [190,191] are limiting factors for the therapeutic effects *in vivo*. Since combination therapy is widely adopted in bacterial treatment, developing synergistic modalities for bacteria elimination has enormous prospects in biomedical applications. The advantages of the two combined treatment methods complement and reinforce each other, leading to an effect of ''1 + 1 > 2''. Consequently, integrating multiple antibacterial mechanisms shortens the time to antibacterial onset, improves the antibacterial efficiency, and reduces the dose of antibacterial agents. Synergistic photothermal antimicrobial therapy primarily involves photodynamic–photothermal therapy, chemo-photothermal therapy, and nitric oxide (NO)–photothermal therapy.

Antibacterial Photothermal Therapy (PTT) - Photodynamic (PDT)

Photothermal-Photodynamic antibacterial therapy combines PTT and photodynamic therapy (PDT) that can kill bacteria with high temperatures and reactive oxygen. Antibacterial PTT-PDT synergism reduces cells' activity through PTT-induced local hyperthermia, increases cell sensitivity to the ROS generated through PDT, and inactivates the cells.[192] Several studies proposed synergistic models following the principles of cost-efficiency and biocompatibility. The QCS/Ag/CoP nanoplatforms demonstrated fast and efficient antibacterial properties while nontoxic to mammals. Moreover, the QCS/Ag/CoP nanocomposites inactivated greater than 99.6% *S. aureus* and *E. coli* at very low concentrations (50 μg/mL) within 10-15 min due to the synergistic effects of the components. Ag enhanced the photocatalytic and photothermal effects of CoP, and the QCS coating improved the water dispersibility to provide better contact between the antiseptics and bacteria.[193] Carbon-based materials with good biocompatibility and environmental-friendly were considered antibacterial agents for the synergism. For instance, the CuS NPs modified on the surface of GO improved PDT efficiency under NIR laser irradiation.

Preprints (www.preprints.org) | NOT PEER-REVIEWED | Posted: 16 May 2023 doi:10.20944/preprints202305.1106.v1

Furthermore, the antibacterial activities of GO, GO@CuS, were less than the try-modal synergistic GO-Tobramycin (Tob) and GO-Tob@CuS nanoplatforms with excellent photothermal conversion capabilities and efficiency against the antibiotic-resistant Pseudomonas aeruginosa (*P. aeruginosa*) and *S. aureus* models [194]. However, the registered toxic effects limited their further implementation.[195] Benefiting from the excellent absorption with NIR, carbon dots (CDs) exhibit a competitive NIR laser-induced photothermal effect which supports directly killing bacteria through hyperthermia from PTT.[113] Since the CDs' antibacterial activity was considered insufficient, the combination of copper ions with NIR-emitting CDs (RCDs) as (Cu-RCDs) and quaternary amino compounds (QACs) as (Cu-RCDs-C_{35}) achieved a better antibacterial effect against Gram-positive and -negative bacteria as tri-modal (photothermal, photodynamic and quaternary ammonium salts) synergistic platforms.[196]

To potentiate the noble metals, such as gold, silver, and palladium or the polyphenolic substances, such as Curcumin (Cur), usually considered photothermal antibacterial agents, loading on small molecules or macromolecule carriers to form nano-agents was considered. For instance, mesoporous silica-modified AuNRs used as carriers loaded Cur constructed a multifunctional composite antibacterial nanosystem (AuNRs@Cur) with significantly improved PTT-PDT antibacterial effects of each incorporated photosensitiser and insignificant cytotoxicity and haemolytic activity.[197] However, noble metals are imperfect due to their intrinsic features, such as poor photostability and biocompatibility, complicated preparation, high cost, and low antibacterial efficiency *in vivo.* Therefore, an alternative such as MoS2/ICG/Ag^+NIR was proposed as another tri-modal synergistic combination PTT/PDT/chemotherapy treatment group with better *in vivo* results: the survival rates of both S. aureus and E. coli were close to zero, indicating that MoS_2/ICG/Ag had the best broad-spectrum antibacterial activity under NIR light irradiation at 808 nm.[156] In the case of combined MoS_2 and TiO_2, within transition metal sulfides/ TiO_2 nanofibers platform (MoS_2/TiO_2 NFs), the photothermal effect of the 3D/2D heterostructure (MoS_2/TiO_2 NFs) significantly improved with a rapid increase in the local temperature to above 50 ^{0}C to inactivate the bacterial proteins. The co-irradiation and oxidase-like synergistic antibacterial platform also increased the permeability of bacterial cell membranes via PTT to increase the membrane permeability for VIS/NIR-activated ROS and lead to bacterial oxidative stress, serious leakage of bacterial contents, peroxidation of the bacterial antioxidants, and eventually death of bacteria. The platform effectively promoted *S. aureus*-infected wound healing while proving negligible haemolytic and cytotoxicity to mammalian cell lines.[198] Meanwhile, other studies used copper sulfide nanoparticles (CuSNPs) as a new class of low-cost PTT and PDT materials with a strong local thermal effect and a large amount of ROS under NIR irradiation that could cause bacterial oxidative damage.[199] Enhancing the antioxidant effect *in vitro* and *in vivo* via a synergistic local PTT-PDT was possible with AgNPs as PAM–PDA/Ag@AgCl [200] and (AgNPs@TA) hydrogels.[201] Furthermore, some antibacterial treatment platforms, photothermal-nanozymes, combined nano-enzymes with peroxidase-like catalytic activity and photothermal effects for antibacterial therapy. IONPs employing synthesized iron oxide (Fe_3O_4) nanoparticles have good biosafety, excellent photothermal conversion ability and peroxidase-like catalytic activity. The production of •OH in a slightly acidic environment achieves specific bactericidal effects and increases the sensitivity of bacteria to heat, thus synergising the PTT.

Interestingly, the reactions stimulated one another, as demonstrated by the excellent antibacterial rate of *E. coli* and *S. aureus in vitro*. *In vivo* study on S. aureus-infected wounds of mice demonstrated that IONPs effectively promoted the healing and the clinical potential as anti-infection therapy.[94] Anti-infection therapy based on enhanced photocatalytic bactericidal activity could be achieved with nanocomposite hydrogels, which showed excellent photothermal properties. The resultant effect was attributed to the combination of polydopamine (PDA) and the natural antioxidant tannic acids (TA), respectively, as demonstrated *in vivo* on the *S. aureus* and *E. coli* co-infected skin wound model. Nanocomposite hydrogel incorporated polydopamine (PDA) for biocompatibility and adhesion. In the case of nano-catalysed hydrogels with an activated infection microenvironment response, polyvinyl alcohol as a scaffold and MXene/CuS bio-heterojunction for PTT-PDT synergistic effects, the hyperthermia and under NIR light generated single oxygen and

Preprints (www.preprints.org) | NOT PEER-REVIEWED | Posted: 16 May 2023 doi:10.20944/preprints202305.1106.v1

hydroxyl radicals induced good antioxidant and antibacterial properties. This approach supported the enhancing phototherapeutic effects in wound infections treatment.[202] Remarkably, infections are caused by aerobic and anaerobic bacteria, and research efforts are focused on related solutions. For instance, in a hypoxic environment *in vivo*, porphyrin from designed macromolecular compounds (e.g., TMPyP, TMPyP/$(CB[7])_4$ [203] TP-Por CON, TP-Por CON@BNN6 [139] could be reduced to phlorin by some facultative anaerobic bacteria with strong reduction ability, such as *E. coli* and *Salmonella typhoid* and act via PTT as good antibacterial. However, in an aerobic environment where aerobic bacteria such as *Bacillus subtilis* and *P. aeruginosa* did not reduce, TMPyP was a typical photosensitiser that could effectively kill bacteria through PDT. Therefore, in one environment and simultaneously, the best porphyrin compound may play the synergistic PTT–PDT effect to improve the antibacterial effect and reduce the side effects of a single treatment while having good biocompatibility. Moreover, AgNPs combined with GO and exposed to NIR irradiation exhibited increased photothermal activity, generating ROS and disrupting the microbial membrane in *E. coli* and *Klebsiella pneumoniae*.[122] A simple one-pot hydrothermal process successfully synthesised a flower-like CuS/GO hybrid. GO operated as a perfect electron acceptor, transported the photogenerated electrons from CuS, and efficiently suppressed the recombination of the hole–electron pairs, thus enhancing the photocatalytic property. Moreover, the CuS and GO structural characteristics also improved the hybrid's photocatalytic functioning. Consequently, the synergistic photothermal-photocatalytic-releasing Cu^{2+} effects within the CuS/GO-based nanosystem contributed to significant antibacterial efficacy under NIR irradiation for 15 min. Furthermore, the hybrid presented pronounced biocompatibility.[204]

Antibacterial Photothermal Therapy (PTT) - NO

NO–photothermal antibacterial therapy combines photothermal agents (PTAs) with NO donor materials for higher bactericidal efficiency.[179] NO has been recognized as a broad-spectrum antibacterial agent with various MOAs, such as inducing lipid peroxidation to damage bacterial membranes, enhancing the RNS production to perturb bacterial metabolisms, or triggering severe oxidative stress for DNA cleavage.[205] Zhao *et al.* [206] combined SNOs with thiolated graphene (TG) and 4-mercaptophenyl boronic acid and added the composite on the surface of TG-NO to achieve one new biocompatible combination, the TG-NO-B. The boric acid groups in TG-NO-B are covalently linked with the bacterial lipopolysaccharide units of bacterial cells and their biofilm matrix. They conferred reasonable specificity *in vivo* and *in vitro* for Gram-negative bacteria. Moreover, intermittent laser irradiation (30 s every 5 min) allowed a NO-controlled release mechanism. Therefore, TG-NO-B significantly improved antibacterial efficiency and reduced adverse side effects on surrounding healthy tissues. Also, a controllable NO release was observed with Fe_3O_4@PDA@PAMAM@NONOate under intermittent 808 nm laser irradiation. The Fe_3O_4@PDA@PAMAM-G3 expressed a concentration-dependent photothermal effect and high photothermal stability with an accelerated NO release under NIR through PTT for anti-*E. coli* and *S. aureus* effects. However, the difference in the NO-releasing activity may be caused by the additional outer membrane barrier of Gram-negative bacilli making them less sensitive to NO. One more practical approach is the excellent magnetic properties of Fe_3O_4@PDA@PAMAM@NONOates, which may be a way of fast complete bacterial removal *in vitro* by the external magnet.[207] The controllable synergistic PTT/NO activity of the MoS_2-BNN6 platform resulted in timely and efficient antibacterial effects against ampicillin-resistant *E. coli*, heat-resistant *Escherichia faecalis* (*E. faecalis*), and *S. aureus*. Notably, the platform worked to selectively enhance oxidative/nitrosative stress and even DNA damage, accelerate glutathione oxidation and subsequently reduce the usage of ROS/RNS generated in bacteria.[208] Being effective even at low concentrations proved to be one crucial asset. In the case of GNS/HPDA-BNN6, the synergistic PTT-NO effectively destroyed bacterial biofilms even at concentrations smaller than 200 mg/ml. The gold nanostar/hollow dopamine Janus nanostructure provided photothermal activity and accurate NIR light-controlled NO release for a strong antibacterial effect at 200 mg/ml via cellular membrane damages, leakage of intracellular components and interference with the bacterial metabolism by up or downregulating genes.[209]

Preprints (www.preprints.org) | NOT PEER-REVIEWED | Posted: 16 May 2023 doi:10.20944/preprints202305.1106.v1

Since varying the nanocomposite ratios within a platform plays an essential part in antibacterial efficacy, attention was paid to this controllable aspect. In the case of BDPNO@PEG-b-PCL micelles, the efficiency changed with the feeding ratios of PEG-b-PCL and BDP-NO. For instance, only NP-4 or NP-5 (1-5 levels) under NIR resulted in evident structural changes, fissures in bacterial membranes, and following cytoplasmic outflow. The BDP-NO nanoparticles indicated a controllable antibacterial effect via NO release, PTT, or a synergistic NO-PTT. Notably, the nanoplatforms with NIR-responsive NO generation and PTT, besides promoting NO penetration into the bacterial cell upon the PTT-induced bacterial wall damages, could dissolve and remove mature biofilms and, through the released NO, modulate the inflammatory immuno-response to reduce tissue damage. Therefore, the synergism NO–PTT proved its antibacterial efficiency on the MRSA-infected skin wound models.[178]

Antibacterial Photothermal Therapy (PTT) - Chemodynamic therapy (CDT)

Chemo-photothermal antibacterial therapy combines PTT with chemical drugs such as metal ions and antibiotics. In this respect, temperature-responsive nanostructures are used as carriers for effective antibacterial therapy if they possess satisfactory biocompatibility, encapsulate antibiotics entirely and securely, combine easily as nanoplatforms, release the encapsulated antibiotics quickly under NIR, and synergise PTT-CPT antibacterial activity. The PTT-Antibiotics mechanism of action (MOA) interferes with the integrity of bacterial membranes thermally and chemically. PTT-CPT synergism may positively influence the outcomes of phototherapy in two ways:

(1) PTT is assisted by CPT by reducing the drug dose, side effects, and drug resistance, and

(2) CPT is combined with PTT by reducing therapy time to protect the normal cells. Several solutions were proposed based on the incorporated antibacterial drugs or nano-enzymes.

The synergetic effects between zeolite imidazole framework-8 and humic acid (HA) (ZIF-8) (HuA@ZIF-8) under NIR light promoted the controlled release of Zn^{2+} ions with antimicrobial activity against *S. aureus* and *E. coli*. ZIF-8 acts as a pH-sensitive vehicle for drug delivery in antibacterial applications. Interestingly, ZIF-8 could be degraded in bacteria-infected areas because of the acidic environment; therefore, it can be incorporated with antibiotics into NIR/pH dual-stimuli-responsive nanoplatforms for the controlled release of an antibacterial drug.[210] Real-time antibacterial drug monitoring was observed with IMP/IR780@TRN nanospheres, comprising imipenem (IMP, a broad-spectrum antibiotic) and IR780 (a photosensitiser molecule. Controllable NIR laser released IMP at the infection site induced cell wall formation inhibition, while the PTT-induced damages to the bacterial membrane effectively killed *E. coli* and *MRSA*.[211] One excellent strategy is to use b-lactam antibiotics to destroy L-forms (b-lactam antibiotics resistant bacteria) cell walls before PTT: it starts with the disruption of the bacterial cell wall by amoxicillin (AMO) and is followed by PTT. Once such nanoplatform is Pd–Cu/AMO@ZIF-8, PCAZ, incorporated ZIF-8 loaded with Amoxicillin (AMO) and showed significant antibacterial effects *in vitro* and *in vivo* (in vitro inhibition rates of S. aureus and P. aeruginosa 99.8% and 99.1%, respectively) and destroyed many biofilms under NIR. The significantly less infiltration of inflammatory cells, intact epidermis, and fewer fibrous cells indicated the progressive wound healing facilitated by accelerated drug release in the wounds' acidic environment and under NIR.[84] Strong NIR absorbance associated with excellent particle size uniformity, like in CuS@Van and cCuS@Van nanoplatforms, allowed more than a simple synergistic interaction. The low-cost, easy-to-prepare, biocompatible nanocomposites comprising CuS NPs and vancomycin (Van) presented a tri-modal photokilling solution as a potential vancomycin-resistant pathogenic bacteria ablation method. Based on CPT-PTT-PDT, the nanoplatforms expressed effective antibacterial capability and rapid infection regression *in vitro* and *in vivo*.[212]

CDT reagents with potent catalytic character have been applied in the infected wound treatment [191], while nanoenzyme-based chemodynamic therapy (CDT) has shown tremendous potential in treating bacterial infections. However, the CDT antibacterial efficacy is severely limited by the catalytic activity of nanoenzymes or the infection microenvironments such as insufficient hydrogen peroxide and over-expressed glutathione (GSH). Therefore, synergistic combinations are considered anti-infective therapies.[213] For instance, Zhu *et al.* [214] described cationic chitosan@ Ruthenium dioxide hybrid nanoenzymes for photothermal therapy enhanced CDT in multidrug-resistant

Preprints (www.preprints.org) | NOT PEER-REVIEWED | Posted: 16 May 2023 doi:10.20944/preprints202305.1106.v1

bacterial infection. CHFH (CuS_{NPs}-HA-Fe^{3+}-EDTA hydrogel) is a bacteria-triggered multifunctional hydrogel constructed for low-temperature photothermal sterilisation and high-efficiency integrated localized chemodynamic therapy (L-CDT). The CuSNPs act as photothermal agents for low-temperature photothermal therapy (LT-PTT). The network of hyaluronic acid (HA) and Fe^{3+}-EDTA complexes allow bacteria to accumulate on the surface where the secreted hyaluronidase decomposes the HA and release Fe^{3+} to be reduced into Fe^{2+} in the bacteria microenvironment. Integrating short-range L-CDT and LT-PTT for sterilisation improved the antibacterial efficiency while minimizing the damage to normal tissues. Furthermore, the CHFH in a band-aid is a potential clinical application, effectively promoting the *S. aureus*-infected wound healing process *in vivo*.[215] Simultaneously introduced indocyanine green photosensitisers and AgNPs onto the surface of MoS_2 nanosheets for chemo/photothermal/photodynamic tri-mode combined antibacterial therapy.[156] Another versatile hybrid nanoenzyme was constructed by grafting ultrasmall CuO_2 nanodots onto the hydrangea-like MoS_2 nanocarriers for synergistic PTT/CDT dual-mode antibacterial therapy. The MoS_2 /CuO_2 nanoenzymes' evaluation revealed better antibacterial MOA through an improved photonic hyperthermia catalytic activity and ROS-based effect by redox. The induced disturbed homeostasis was possible due to the co-catalysis-boosted peroxidase-mimic activity, H_2O_2 self-supplying ability and GSH-depleting property by oxidisation of GSH to GSSG by both Cu^{2+} and Mo^{6+} within the system. The *in vitro* 99% antibacterial efficacy against *S. aureus and E. coli* was reached at 50 μg mL^{-1} and 100 μg mL^{-1}, respectively. The possible cause of this difference was the relatively thinner and more porous cell membrane of *S. aureus*. The studies indicated that, *in vitro* and *in vivo*, NIR-MoS_2/CuO_2 caused severe damage and more intense bacteria collapse and deformation, effectively eliminating *S. aureus* and *E. coli*, thus showing strong PTT/CDT dual-mode synergistic antibacterial properties while good biosafety and nontoxicity. The MoS_2 /CuO_2 nanoenzymes proved good biosafety and nontoxic effects on the NIH_3T_3 cells and promoted cell growth, thus promising further applications.[216] Developing intelligent nanotherapeutics for antibacterial therapy is supported by a satisfactory *in vitro* and *in vivo* bactericidal activity of a novel infection microenvironment-responsive PTT/CDT synergistic nanoplatform $Cu_{1.94}S$@MPN constructed by encapsulating $Cu_{1.94}S$ with Fe(III)/tannic acid (TA) based metal-polyphenol networks (MPN) nano-shells. The excellent inherent photothermal conversion property of MPN and continuous Cu(I) ions supply via reducing Cu(II) with TA achieved self-boosted synergistic PTT/CDT with extraordinary photothermally and photothermally enhanced chemodynamic efficiency.[217] Functionalisation of carbon dots (CD) as a nanoplatform for synergistic antibacterial chemodynamic and photothermal therapy was proposed. CD/iron oxychloride nanosheets (CD/FeOCl NSs) catalyst with hydrogen peroxide (H_2O_2) induced CDT, while the coating of inorganic CDs and NIR organic polyethylene glycol PEG mediated the PTT. The developed FeOCl@PEG@CDs NCs employed the Fe(II)'s improved selectivity toward ·OH generation. The efficient synergistic CDT/PTT in the FeOCl@PEG@CDs NCs plus H_2O_2 and FeOCl@PEG@CDs NCs plus laser groups significantly deformed the bacterial surface and inhibited and killed the bacteria. The good *in vitro* and *in vivo* antibacterial results are the attributes of the combined CDT effect of FeOCl and the PTT effect of CDs. Moreover, the CDs' excellent biosafety and high photostability increase the FeOCl@PEG@CDs NCs nanocomposite's potential as antibacterial agents and wound microenvironment regulators.[190] Significantly, self-assembled microsphere hydrogel scaffold (SMHS) regulating the diabetic wounds' microenvironment via synergistic PTT/CDT might play an essential role in their healing process. SMHS+NIR can combine the physical (photothermal therapy) and chemical (drug delivery) mechanisms to increase the anti-inflammatory response, angiogenesis and tissue remodelling significantly and simultaneously. Two kinds of hydrogel microspheres with opposite charges were independently prepared for SMHS: chitosan methacryloyl (CS) and hyaluronic acid methacryloyl (HA). The positively charged CS microspheres were loaded with PEGylated black phosphorus nanosheet (BP) nanosheets, while the negatively charged HA microspheres were loaded with basic fibroblast growth factor (bFGF). The BP provide an efficient photothermal response under NIR irradiation and naturally degrades into $PO4^{3-}$ or $HPO4^{2-}$ in a physiological environment while tissues friendly. The BP@CS and NIR irradiation may be the main contributors to the bactericidal effect via membrane rupture, as per the investigation of SMHS against Gram-negative *E. coli* and Gram-positive *S. aureus*. Moreover, chitosan provides some anti-bacterial effects, and BP-PEG can strengthen antimicrobial activity via a photothermal effect. The *in vivo* study showed several promising outcomes in the group of SMHS+NIR: an early enhanced local angiogenesis (day 3), better re-epithelialisation (day 14), a typical near-to-normal histological architecture, and ameliorated inflammatory environment promoted by the macrophage polarisation to the M2 subtype.[218] Still, overcoming the PTT-related side effects is crucial. Therefore, a bimetal-doped nanosheet (FeS@Cu2O) was proposed. Fabricated via a hydrothermal method, it integrates photothermal, photodynamic and chemo-dynamic properties. FeS and Cu_2O are considered ideal photothermal agents individually due to electron-hole generation and relaxation under NIR. However, FeS@Cu2O releases Fe2+ and Cu+ and owns superior photocatalytic ability for PDT and CDT. Therefore, the nanocomposites induce efficient antibacterial effects against *E. coli* and *S. aureus* via local hyperthermia and endogenous ROS as a versatile multimodal synergistic therapy for sterilisation.[219]

Other combinations

Sonodynamic therapy (SDT) combines acoustic sensitizers and low-intensity ultrasound to activate the sensitizers, focus the ultrasound energy deep at the infected tissue, produce mechanical damage via cavitation, sonoporation [220], and cytotoxic ROS via sonoluminescence for a bactericidal effect. Moreover, the sonoporation can increase the cell membrane permeability, thus increasing the transmembrane drug transport.[221] Since sonoluminescence at this stage is difficult to regulate and causes toxic or other side effects on healthy tissues, combining SDT with PTT may synergise the therapeutic effects and diminish the damage to normal tissues. Most photosensitive agents have the potential to act as acoustic sensitizers. For instance, silver peroxide NPs (Ag2O2 NPs) are a potential antibacterial drug due to good photothermal and acoustic sensitizer properties able to produce ROS and penetrate deeper into infected tissues with more treatment specificity.[222] To improve the antimicrobial specificity, PTT combined **immunotherapy** as an antibacterial option was observed as advanced immunoconjugates. They are adjuvants or antigens altered as antibacterial agents to facilitate complex immune responses via bacterial toxicity and bacterial antigens recognition.[223] One example is the nano-neuro-immune blockers (NNIBs) obtained by modifying an immune escape outer membrane on the Au nanocages' surfaces (AuNCs).[224] NNIBs present specificity towards the toxins of *S. pyogenes*, neutralize streptolysin S (SLS), unblock the neutrophils production and enhance the host's immune response to the bacterial infection. Also, the AuNCs' good photothermal activity effectively induces acute inflammatory response with positive feedback on the immune response. Furthermore, a photoexcited hydroxyapatite (Hap)/nitrogen-doped carbon dot (NCDS) modified GO heterojunction film (GO/NCD/Hap) improved the photocatalysis and photothermal effects with beneficial consequences on tissues, such as *in vivo* vascular injury repair.[225] The electron transfer synergises PDT and PTT through immune therapy to better treat bacterial infections.[226] Therefore, the combination of PTT and SDT or immunotherapy is anticipated to have more application prospects due to the minimally invasive nature and higher antibacterial effect.

In conclusion, combining photothermal therapy with other photodynamic treatments is a promising direction to play a synergistic role in improving the antibacterial efficiency, shortening the antibacterial time, and reducing the side effects of different methods on the human body when used alone. One important application is wound healing, particularly diabetic and slow-healing surgical wounds extremely susceptible to drug-resistant bacterial infections.

4.3. Cutaneous wounds

The worldwide wound care marketplace of USD 20.8 billion in 2022 is anticipated to reach a compound annual growth rate (CAGR) of 5.4% by 2027 (USD 27.2 billion). [171] *Wound healing* is a complex process employing inflammation, proliferation, epithelialisation, and remodelling at haemostasis, [26] hindered by bacterial infection, especially in chronic wounds, such as diabetic foot ulcers, non-healing surgical wounds, or peripheral vascular diseases.[227–229] Therefore, efforts focused on solutions that can protect wounds by defeating antibiotic-resistant strains and promoting

Preprints (www.preprints.org) | NOT PEER-REVIEWED | Posted: 16 May 2023 doi:10.20944/preprints202305.1106.v1

the healing of either superficial (wavelengths below 400nm) or deep (400 to 850nm) cutaneous wounds.

One functionalized water-soluble photothermal agent modified with quaternary ammonium salts (RT-MN) based on electrostatic adsorption was proposed for photothermal antibacterial treatment. The principle of electrostatic interaction facilitates the RT-MN molecules' binding to the bacterial membranes to assist the photothermal antibacterial treatment. Since RT-MN is positively charged, whereas MRSA and E. coli are negative, it can bind to bacteria through electrostatic adsorption. Moreover, besides exceptional photothermal conversion ability (irradiation of lasers of 808 nm, 150 μM the optimal concentration), RT-MN possesses a selective bactericidal effect at high temperatures. RT-MN +NIR destroyed the bacterial membrane and effectively inhibited the growth of *MRSA* and *E. coli*. Subsequently, the in vivo antibacterial ability was successfully demonstrated in an MRSA-infected mouse skin wound model. The good biocompatibility of RT-MN combined with the NIR irradiation successfully reduced the sizes of infected wounds and facilitated healing via an anti-inflammatory response and increased collagen secretion.[230] Similarly, NIR-irradiated Au@CD-based membranes effectively eradicated bacteria at the wound site, reduced the risk of bacterial infection, suppressed inflammation, and improved collagen deposition and angiogenesis, facilitating wound closure via photothermal antimicrobial effect. The healing platform comprised a PVA membrane, which embedded AuNPs and N,S-CDs via electrospinning. The CDs as surface decorations conferred improved photothermal conversion efficiency, photostability, and biocompatibility to the Au@CD compared to the parent AuNPs. The membranes presented excellent biocompatibility and photothermal antimicrobial activity against S. *aureus* and *E. coli* (99 + % inactivation of both pathogens under NIR irradiation) *in vitro* and *in vivo*.[231] As mentioned, wound dressing hydrogels have attracted much attention due to the interconnected microporous networks, which can maintain a humid microenvironment and promote the absorption of wound exudate and the oxygen transmission. The hydrogels effectively improved the permeability of bacterial membranes, ruptured the bacterial membrane, and allowed oxidative stress and serious protein leakage, thus, bacterial death. Importantly, due to the negligible side effects, this system has great clinical potential for sterilisation through the combination of PTT and PDT. Therefore, nanocomposite hydrogels with antibacterial and antioxidant capabilities have great application potential in treating infected skin wounds. For instance, introducing anils as antibacterial agents into polyvinyl alcohol (PVA) hydrogel was a good choice to achieve the rapid antibacterial therapeutic effect. An antibacterial platform (DPVA hydrogel) mainly derived from the photothermal effect of N-(2,4-dihydroxybenzylidene)-4-aminophenol (DOA) was tested for the efficient and rapid treatment of drug-resistant bacterial infections in skin wounds. An excited state proton transfer (ESIPT) process as nonradiative transitions was utilized to promote the photothermal effect and increase the local temperature to 55^{0}C within 10s under irradiation. *In vitro*, evaluations showed a broad-spectrum antibacterial ability against Staphylococcus aureus and Escherichia coli (antibacterial rate 99%) and Methicillin-resistant Staphylococcus aureus and Enteroinvasive Escherichia coli (about 1%. bacterial survival rate). *In vivo* wound healing in mice showed that DPVA hydrogel could effectively cure *MRSA*-induced whole-layer wound infections within 100 seconds of irradiation, opening a new way to develop antibacterial dressing with rapid response and convenient fabrication.[51] Also notable is the 98% wound healing rate with complete re-epithelisation after a 10-day therapy with the MXenes@PVA plus NIR. MXenes@PVA hydrogel was effective against *S. aureus* and presented high toughness, anisotropy, and antimicrobial properties, thus a promising antibacterial dressing for wound healing. Other composites Ti_3C_2Tx/Ag_3PO_4, Ti_3C_2Tx/MoS_2, Ti_3C_2Tx/Bi_2S_3, Ti_3C_2Tx/Ag, and Nb_2C also presented potential *in vivo* wound healing capabilities.[96] Furthermore, the BSA@MPN, produced by Fe3+/ EGCG-based self-assembly using BSA as the nanoreactor and colloidal stabilizer, possessed excellent photothermal-related bactericide, and macrophages M1-to-M2 phenotypic conversion-related anti-inflammatory effects due to the photothermal property and pH-responsive degradability of Fe3+/EGCG-based MPN. Next to the biocompatibility and biosafety properties, the *in vitro* and *in vivo* antibacterial and anti-inflammatory effects are imperatives to wound healing.[170] Since wound healing involves wound management, developing an ideal hydrogel-based dressing is essential. However, producing a smart and dynamic hydrogel to adjust to the wound-healing process is still challenging. The dressing needs to have complex properties to facilitate healing.[232,233] Both elasticity and antibacterial properties were obtained for a GO hybrid hydrogel scaffold prepared by injecting benzaldehyde and cyanoacetate group-functionalized dextran solution containing GO into a pool of histidine. This scaffold also showed an enhanced cargo due to the thermosensitive C double bond breaking under NIR light and at a high temperature.[234] Since GO possesses obvious photothermal behaviour, it was also considered for loading an electrospun hyaluronic acid membrane. The proposed wound dressing loaded with GO and ciprofloxacin presented a bactericidal effect based on the synergistic action of the antibiotic and NIR-mediated hyperthermia.[235,236] A similar synergistic effect was observed in another NIR-responsive rGO hybrid cryogel with excellent properties: rGO photothermal effect allowed the cryogel heating and subsequent swelling followed by the encapsulated drug release.[237] The elevated local temperature by the photosensitiser graphene denatures the microbial proteins, which decreases the viability of the pathogenic microorganisms, MRSA included.[236] Furthermore, combining PTT and PDT was considered. Chitosan oligosaccharide functionalized graphene quantum dots (GQDs-COS) with short-term exposure to 450 nm visible [238] and a nanocomposite poly(vinylidene) fluoride membrane with TiO_2 NPs as the outer shell and NaYF4:Yb,Tm nanorods as the core doped with nanosized GO as a photothermal agent[169] were proposed. The suggested MOA is a complex PTT-PDT synergism initiated by PTT, completed by PDT and manifested by increased electrostatic attraction between the NPs and the bacteria, irreversible disintegration of bacterial cytomembranes, leaked cytoplasm, oxidized vital subcellular targets, disturbed bacterial homeostasis, and bacterial death. Therefore, the GO hybrid hydrogel scaffolds could be used as multifunctional wound dressings because of their photothermal antibacterial, adjustable mechanical, and angiogenesis promoter properties. *In vivo* (5 days of treatment on mice) results suggested that NIR laser-assisted MoS_2/CuO_2 nanoenzymes effectively eliminated *S. aureus* infection by a PTT/CDT dual-mode synergistic antibacterial result, finally achieving adequate wound healing. The results confirmed the MoS_2/CuO_2 potential as an effective PTT agent for future biomedical applications.[216] Chang *et al.* demonstrated the successful PPT-PDT synergism as a potential modality in treating of infected skin wounds. The proposed functional wound dressing combined an enzyme-crosslinked hyaluronic acid-tyramine (HT) hydrogel and antioxidant and photothermal AgNPs capped with tannic acids (AgNPs@TA). The natural antioxidant tannic acids (TA) acted as reducing and stabilizing agents to facilitate the synthesis. The HTA hydrogel is biocompatible and easy to use, while AgNPs@TA significantly enhanced the photothermal, antioxidant, antibacterial, adhesive, and haemostatic abilities of the resulting nanocomposite. *In vivo,* studies on the *S. aureus* and *E. coli* co-infected mouse skin wound models showed that HTA0.4 (containing 0.4 mg/mL AgNPs@TA) hydrogel combined with NIR radiation highly reduced inflammation, helped angiogenesis, and enhanced the healing process. Therefore, the antibacterial and antioxidant AgNPs@TA is a promising wound dressing.[201] DPVA hydrogel was also evaluated for its efficient photothermal antibacterial effects with potential application as wound dressing for infected wounds. *In vitro* and *in vivo* studies showed excellent antibacterial effects against Methicillin-resistant *S. aureus* and *Enteroinvasive E. coli*, explained by the completely disrupted bacterial structure due to the generated PTT induced hyperthermia. Notably, the new epidermal tissue formation indicated a healing process.[51] Angiogenesis and collagen deposition as healing steps were facilitated by a biocompatible adhesive nanocatalytic hydrogel of polyvinyl alcohol (PVA) scaffold, MXene/CuS bio-heterojunction, and polydopamine (PDA). The MXene/CuS's photothermal effect and the NIR light generated oxygen and hydroxyl radicals explained the good antioxidant and antibacterial capacity, thus the in vivo good skin regenerative ability through bactericidal, angiogenesis and collagen deposition promoter. The proposed approach supports further research for nanocatalysed hydrogels with an infection microenvironment-induced response to treat infected wounds through enhanced phototherapeutic effects.[202,239] Ag NPs-incorporated quaternized chitin nanocomposite was constructed by in situ synthesis method, for application in biofilms-infected wound treatment, for the first time. Ag^+ was in situ reduced to Ag NPs stabilized by catechol functionalized quaternized chitin (DQC) micelle to

Preprints (www.preprints.org) | NOT PEER-REVIEWED | Posted: 16 May 2023 doi:10.20944/preprints202305.1106.v1

form DQCA in a green way, without extra reductant or UV irradiation. The rationally designed DQCA would be endowed with bacterial targeting, sterilisation effects of cationic groups and Ag NPs, and superior photothermal combined bactericidal and antibiofilm activities. Furthermore, the DQCA solution was injected into a mouse full-thickness *S. aureus* biofilms-infected wound to demonstrate the application prospect of wound healing. This study will provide a new multifunctional silver/polysaccharide candidate for treating biofilm-infected wounds.[78] *In vitro* and *in vivo* studies presented a porphyrin-based covalent organic framework, TP-PorCON@BNN6, as a triple antibacterial model, with good biocompatibility, negligible toxicity, and multifunctional biological activity. It promoted bacterial apoptosis by producing ROS, hyperthermia, and releasing NO, via a synergistic effect of PDT, PTT, and GT. *In vivo,* antibacterial activity was quantified on S. aureus-infected chronic wound healing receiving different treatments (PBS, PDT, PDT + PTT, and PDT + PTT + GT). Accelerated the healing of infected wounds by simultaneously reducing oxidative stress, regulating inflammatory factors, accelerating collagen deposition, and promoting angiogenesis were observed.[139] Other multifunctional antibacterial nanoplatforms could employ PTT, PDT and SDT for guided therapy and rapid healing. For instance, AIE-Tei@AB NVs was designed as a laser-activated "nanobomb" for the multimodal theranostics of drug-resistant bacterial infections. It comprises lipid nanovesicles from the self-assembled aggregation-induced emission (AIE) nanosphere (AIE-PEG1000 NPs) with near-infrared region II (NIR-II) fluorescence emissive, photothermal, and photodynamic properties. Furthermore, the nanobomb combined the excellent pharmacological properties of rapidly released Tei during bubble generation and NV disintegration capacity. Therefore, the in vivo experiments validated the high-performance NIR-II fluorescence, infrared thermal, ultrasound imaging of multidrug-resistant bacteria-infected foci, broad-spectrum eradication of clinically isolated MRSA, MDR E. coli, and MDR Pseudomonas aeruginosa and rapid healing of infected wounds upon intravenous administration of AIE-Tei@AB NVs followed by 660 nm laser stimulation. This multimodal imaging-guided synergistic therapeutic strategy can be extended for the theragnostic of superbugs.[240] Ultimately, intelligent wound dressing intends to regulate the microenvironment by attenuating the inflammation responses, promoting re-epithelisation, granulation formulation, angiogenesis and collagen deposition. The literature strongly suggests that NIR exposure has multifunctional effects and holds enormous potential for wound therapy. In conclusion, the need for two-dimension nanomaterials as promising candidates for wound healing imposes photothermal agents to the forefront. They can provide an efficient photothermal response under NIR irradiation and naturally degrade in a physiological environment, completely harmless to surrounding tissues.

5. Conclusions, challenges, and perspectives

The review presents how nanotechnological progress introduced many new nanomaterials as PTT agents (PTAs), showing good bactericidal activity in controlled nanosystems. Moreover, various methods were presented to target the PTAs' actions to ensure their bacterial specificity and binding to targeted bacteria and not to human cells to improve their concentration in the targeted infected area. However, functionalising PTAs to increase their photothermal efficiency is one of many conditions imposed when fulfilling the essential criteria for future clinical implementation. There are biocompatibility requirements which are vital to a clinically applicable nanosystem. Therefore, the new approaches supported by nanotechnology considered combining PTAs with other materials to improve the antibacterial efficiency and reduce unwanted side effects. The technological outcomes presented here explain the recent applications of PTT to sterilisation through removing bacterial biofilm from different medical surfaces and implants and to rapid healing of infected wounds via molecular implications of PTT alone or in synergistic combinations. Despite the recent *in vivo* progress in PTA-based antimicrobial agents, the transition of these materials from benchtop to bedside still needs to be improved. For instance, in the case of PTAs combined with antibiotics, there is the risk of unpredictable drug distribution and suboptimal local concentration, which may limit its therapeutic effect. This example also explains the need for protocol standardisation as one crucial issue that needs to be addressed in antimicrobial PTAs. However, this desiderate is challenging to

Preprints (www.preprints.org) | NOT PEER-REVIEWED | Posted: 16 May 2023 doi:10.20944/preprints202305.1106.v1

accomplish since there are multiple variables to control simultaneously. It is not easy to consolidate the wide variety of nanomaterials employed at various concentrations, with different power densities and for various amounts of NIR exposure time for the best efficacy and highest safety to the tissues.

Consequently, it is not easy to compare the antimicrobial potency between different PTAs and to enable a better translation into the clinical setup. Notably, only a limited number of studies address the biocompatibility of these photothermal nanomaterials and their stability issues in the tissue environment. Moreover, the scientific community invested significant effort over the past few years to address the challenges, and communicate the results to set future work. For instance, future studies will focus on biosafety to address the PTA's interactions with the immune system, their long-term biosafety, the assessment of potential degradation products and the effects of undesirable diffusion of the nanomaterials. Future studies could focus on more systematic investigations of the PTA's antibacterial mechanisms with the help of *in silico* prediction models. The therapeutic efficiency and efficacy against different types of clinically relevant biofilm-associated infections could be beneficial from the clinical point of view. Eventually, well-structured studies will investigate the pharmacological aspects of dynamics, kinetics, and toxicology for detailed profiles of PTA's. Aspects include administration routes, biodistribution, nanoparticles' metabolism and excretion (clearance), off-target effects of NIR irradiation, cytotoxicity, and interaction with the commensal microbiota.

Regarding the anti-biofilms capabilities, detailed mechanisms about the PTAs' ability to penetrate the biofilm deeply or accumulate at the biofilm site should be considered when developing PTAs. Finally, intense exploitation of the use of natural compounds to decrease manufacturing costs and the negative impact on the environment could be considered. Therefore, nanotechnology must take an essential step towards the large-scale production of synthesised nanomaterials in laboratories for their translation into widespread clinical therapeutic devices. Successful design, characterisation, and transition into the clinical setup will only be possible due to a comparative, interdisciplinary approach involving clinicians, pharmacists, engineers, microbiologists, chemists, and industrial partners.

Author Contributions: Conceptualization, V.D, F.S.I. & C.I.; writing: V.D., J.G. K.H.C, G.G.P, F.S.I., & C.I.; writing—review and editing, F.S.I., C.I..; visualization, G.G.P.&J.G..; supervision, C.I..; funding acquisition, C.I. All authors have read and agreed to the published version of the manuscript.

Funding: V.D., F.S.I. and C.I. acknowledge the support from the grant of the Romanian Ministry of Research, Innovation and Digitalization, CCCDI–UEFISCDI, PN-III-P4-ID-PCE-2020-186 Contract PCE 180/17/02/2021 awarded to C.I. J.G, G.G.P, & C.I acknowledge the support from the European Union's Horizon Europe framework program 2021-2027, under the Coordination and Support Actions, HORIZON-WIDERA-2022-TALENTS-01 (grant agreement - 101087007 – eBio-hub). Funded by the European Union. Views and opinions expressed are however those of the authors only and do not necessarily reflect those of the European Union or European Research Executive Agency (REA). Neither the European Union nor the granting authority can be held responsible for them.

Institutional Review Board Statement: the study did not require ethical approval.

Data Availability Statement: No new data was created.

Conflicts of Interest: The authors declare no conflict of interest.

References

1. https://www.cdc.gov/drugresistance/ar-lab-networks/global.html. Available online: (accessed on
2. Ventola, C.L. The antibiotic resistance crisis: part 1: causes and threats. *Pharmacy and therapeutics* **2015**, *40*, 277.
3. https://www.cdc.gov/drugresistance/biggest-threats.html. Available online: (accessed on
4. https://www.who.int/news-room/fact-sheets/detail/antimicrobial-resistance. Available online: (accessed on
5. Razzaque, M.S. Commentary: microbial resistance movements: an overview of global public health threats posed by antimicrobial resistance, and how best to counter. *Frontiers in Public Health* **2021**, *8*, 629120.
6. Blair, J.M.; Webber, M.A.; Baylay, A.J.; Ogbolu, D.O.; Piddock, L.J. Molecular mechanisms of antibiotic resistance. *Nature reviews microbiology* **2015**, *13*, 42-51.

Preprints (www.preprints.org) | NOT PEER-REVIEWED | Posted: 16 May 2023 doi:10.20944/preprints202305.1106.v1

7. Wright, G.D.; Sutherland, A.D. New strategies for combating multidrug-resistant bacteria. *Trends in molecular medicine* **2007**, *13*, 260-267.
8. Li, W.; Separovic, F.; O'Brien-Simpson, N.M.; Wade, J.D. Chemically modified and conjugated antimicrobial peptides against superbugs. *Chemical Society Reviews* **2021**, *50*, 4932-4973.
9. Neu, H.C. The crisis in antibiotic resistance. *Science* **1992**, *257*, 1064-1073.
10. Costerton, J.W.; Stewart, P.S.; Greenberg, E.P. Bacterial biofilms: a common cause of persistent infections. *science* **1999**, *284*, 1318-1322.
11. Chen, M.; Yu, Q.; Sun, H. Novel strategies for the prevention and treatment of biofilm related infections. *International journal of molecular sciences* **2013**, *14*, 18488-18501.
12. Hetta, H.F.; Ramadan, Y.N.; Al-Harbi, A.I.; A. Ahmed, E.; Battah, B.; Abd Ellah, N.H.; Zanetti, S.; Donadu, M.G. Nanotechnology as a Promising Approach to Combat Multidrug Resistant Bacteria: A Comprehensive Review and Future Perspectives. *Biomedicines* **2023**, *11*, 413.
13. Kwon, H.-Y.; Godman, B. *Pharmaceutical policy, impact and health outcomes*; Frontiers Media SA: 2023; Volume 16648714.
14. Wang, Z.; Koirala, B.; Hernandez, Y.; Zimmerman, M.; Park, S.; Perlin, D.S.; Brady, S.F. A naturally inspired antibiotic to target multidrug-resistant pathogens. *Nature* **2022**, *601*, 606-611.
15. Su, Y.; Yrastorza, J.T.; Matis, M.; Cusick, J.; Zhao, S.; Wang, G.; Xie, J. Biofilms: Formation, Research Models, Potential Targets, and Methods for Prevention and Treatment. *Advanced Science* **2022**, *9*, 2203291.
16. Hussain, S.; Joo, J.; Kang, J.; Kim, B.; Braun, G.B.; She, Z.-G.; Kim, D.; Mann, A.P.; Mölder, T.; Teesalu, T. Antibiotic-loaded nanoparticles targeted to the site of infection enhance antibacterial efficacy. *Nature biomedical engineering* **2018**, *2*, 95-103.
17. Wang, Y.; Yang, Y.; Shi, Y.; Song, H.; Yu, C. Antibiotic-free antibacterial strategies enabled by nanomaterials: progress and perspectives. *Advanced Materials* **2020**, *32*, 1904106.
18. Maillard, J.-Y.; Hartemann, P. Silver as an antimicrobial: facts and gaps in knowledge. *Critical reviews in microbiology* **2013**, *39*, 373-383.
19. Kim, J.S.; Kuk, E.; Yu, K.N.; Kim, J.-H.; Park, S.J.; Lee, H.J.; Kim, S.H.; Park, Y.K.; Park, Y.H.; Hwang, C.-Y. Antimicrobial effects of silver nanoparticles. *Nanomedicine: Nanotechnology, biology and medicine* **2007**, *3*, 95-101.
20. Lansdown, A.B. Silver in health care: antimicrobial effects and safety in use. *Biofunctional textiles and the skin* **2006**, *33*, 17-34.
21. Liao, C.; Li, Y.; Tjong, S.C. Bactericidal and cytotoxic properties of silver nanoparticles. *International journal of molecular sciences* **2019**, *20*, 449.
22. Kumar, R.; Umar, A.; Kumar, G.; Nalwa, H.S. Antimicrobial properties of ZnO nanomaterials: A review. *Ceramics International* **2017**, *43*, 3940-3961.
23. Sánchez-López, E.; Gomes, D.; Esteruelas, G.; Bonilla, L.; Lopez-Machado, A.L.; Galindo, R.; Cano, A.; Espina, M.; Ettcheto, M.; Camins, A. Metal-based nanoparticles as antimicrobial agents: an overview. *Nanomaterials* **2020**, *10*, 292.
24. Dediu, V.; Busila, M.; Tucureanu, V.; Bucur, F.I.; Iliescu, F.S.; Brincoveanu, O.; Iliescu, C. Synthesis of ZnO/Au Nanocomposite for Antibacterial Applications. *Nanomaterials* **2022**, *12*, 3832.
25. Tian, E.-K.; Wang, Y.; Ren, R.; Zheng, W.; Liao, W. Gold nanoparticle: Recent progress on its antibacterial applications and mechanisms. *Journal of Nanomaterials* **2021**, *2021*, 1-18.
26. Zheng, K.; Setyawati, M.I.; Leong, D.T.; Xie, J. Observing antimicrobial process with traceable gold nanoclusters. *Nano Research* **2021**, *14*, 1026-1033.
27. Zhang, Y.; Shareena Dasari, T.P.; Deng, H.; Yu, H. Antimicrobial activity of gold nanoparticles and ionic gold. *Journal of Environmental Science and Health, Part C* **2015**, *33*, 286-327.
28. Fu, G.; Vary, P.S.; Lin, C.-T. Anatase TiO2 nanocomposites for antimicrobial coatings. *The journal of physical chemistry B* **2005**, *109*, 8889-8898.
29. Calabrese, C.; La Parola, V.; Testa, M.L.; Liotta, L.F. Antifouling and antimicrobial activity of Ag, Cu and Fe nanoparticles supported on silica and titania. *Inorganica Chimica Acta* **2022**, *529*, 120636.
30. Ren, G.; Hu, D.; Cheng, E.W.; Vargas-Reus, M.A.; Reip, P.; Allaker, R.P. Characterisation of copper oxide nanoparticles for antimicrobial applications. *International journal of antimicrobial agents* **2009**, *33*, 587-590.
31. Hashem, A.H.; Al Abboud, M.A.; Alawlaqi, M.M.; Abdelghany, T.M.; Hasanin, M. Synthesis of nanocapsules based on biosynthesized nickel nanoparticles and potato starch: Antimicrobial, antioxidant, and anticancer activity. *Starch-Stärke* **2022**, *74*, 2100165.
32. Filipović, N.; Ušjak, D.; Milenković, M.T.; Zheng, K.; Liverani, L.; Boccaccini, A.R.; Stevanović, M.M. Comparative study of the antimicrobial activity of selenium nanoparticles with different surface chemistry and structure. *Frontiers in bioengineering and biotechnology* **2021**, *8*, 624621.
33. Jung, H.S.; Verwilst, P.; Sharma, A.; Shin, J.; Sessler, J.L.; Kim, J.S. Organic molecule-based photothermal agents: an expanding photothermal therapy universe. *Chemical Society Reviews* **2018**, *47*, 2280-2297.
34. Parisi, O.I.; Scrivano, L.; Sinicropi, M.S.; Puoci, F. Polymeric nanoparticle constructs as devices for antibacterial therapy. *Current Opinion in Pharmacology* **2017**, *36*, 72-77.

Preprints (www.preprints.org) | NOT PEER-REVIEWED | Posted: 16 May 2023 doi:10.20944/preprints202305.1106.v1

35. Khalid, M.; El-Sawy, H.S. Polymeric nanoparticles: Promising platform for drug delivery. *International journal of pharmaceutics* **2017**, *528*, 675-691.
36. Zhao, Y.; Jiang, X. Multiple strategies to activate gold nanoparticles as antibiotics. *Nanoscale* **2013**, *5*, 8340-8350.
37. Zafar, A.; Alruwaili, N.K.; Imam, S.S.; Alsaidan, O.A.; Ahmed, M.M.; Yasir, M.; Warsi, M.H.; Alqurain, A.; Ghoneim, M.M.; Alshehri, S. Development and optimization of hybrid polymeric nanoparticles of apigenin: Physicochemical characterization, antioxidant activity and cytotoxicity evaluation. *Sensors* **2022**, *22*, 1364.
38. Liu, Y.; Xiao, Y.; Cao, Y.; Guo, Z.; Li, F.; Wang, L. Construction of chitosan-based hydrogel incorporated with antimonene nanosheets for rapid capture and elimination of bacteria. *Advanced Functional Materials* **2020**, *30*, 2003196.
39. Qiu, Y.; Yu, S.; Wang, Y.; Xiao, L.; Pei, L.; Pu, Y.; Zhang, Y. Photothermal therapy may be a double-edged sword by inducing the formation of bacterial antibiotic tolerance. *Biomaterials Science* **2022**, *10*, 1995-2005.
40. Zhang, L.; Wang, Y.; Wang, J.; Wang, Y.; Chen, A.; Wang, C.; Mo, W.; Li, Y.; Yuan, Q.; Zhang, Y. Photon-responsive antibacterial nanoplatform for synergistic photothermal-/pharmaco-therapy of skin infection. *ACS applied materials & interfaces* **2018**, *11*, 300-310.
41. Wang, B.; Xu, Y.; Shao, D.; Li, L.; Ma, Y.; Li, Y.; Zhu, J.; Shi, X.; Li, W. Inorganic nanomaterials for intelligent photothermal antibacterial applications. *Pharmaceutical Materials for Tumor Imaging and Therapy* **2023**, *16648714*, 79.
42. Abbas, M.; Ovais, M.; Atiq, A.; Ansari, T.M.; Xing, R.; Spruijt, E.; Yan, X. Tailoring supramolecular short peptide nanomaterials for antibacterial applications. *Coordination Chemistry Reviews* **2022**, *460*, 214481.
43. Hamblin, M.R. Antimicrobial photodynamic inactivation: a bright new technique to kill resistant microbes. *Current opinion in microbiology* **2016**, *33*, 67-73.
44. Chen, T.; Gu, T.; Cheng, L.; Li, X.; Han, G.; Liu, Z. Porous Pt nanoparticles loaded with doxorubicin to enable synergistic Chemo-/Electrodynamic Therapy. *Biomaterials* **2020**, *255*, 120202.
45. Krieg, A.M.; Wagner, H. Causing a commotion in the blood: immunotherapy progresses from bacteria to bacterial DNA. *Immunology today* **2000**, *21*, 521-526.
46. Jauffred, L.; Samadi, A.; Klingberg, H.; Bendix, P.M.; Oddershede, L.B. Plasmonic heating of nanostructures. *Chemical reviews* **2019**, *119*, 8087-8130.
47. Beyth, N.; Houri-Haddad, Y.; Domb, A.; Khan, W.; Hazan, R. Alternative antimicrobial approach: nano-antimicrobial materials. *Evidence-based complementary and alternative medicine* **2015**, *2015*.
48. Ju, Q.; Chen, X.; Ai, F.; Peng, D.; Lin, X.; Kong, W.; Shi, P.; Zhu, G.; Wang, F. An upconversion nanoprobe operating in the first biological window. *Journal of Materials Chemistry B* **2015**, *3*, 3548-3555.
49. Xu, J.-W.; Yao, K.; Xu, Z.-K. Nanomaterials with a photothermal effect for antibacterial activities: an overview. *Nanoscale* **2019**, *11*, 8680-8691.
50. Bai, X.; Yang, Y.; Zheng, W.; Huang, Y.; Xu, F.; Bao, Z. Synergistic Photothermal Antibacterial Therapy Enabled by Multifunctional Nanomaterials: Progress and Perspectives. *Materials Chemistry Frontiers* **2023**.
51. Yao, W.; Deng, T.; Huang, A.; Zhang, Y.; Li, Q.; Li, Z. Promoting photothermal antibacterial activity through an excited-state intramolecular proton transfer process. *Journal of Materials Chemistry B* **2023**.
52. Xu, D.; Li, Z.; Li, L.; Wang, J. Insights into the photothermal conversion of 2D MXene nanomaterials: synthesis, mechanism, and applications. *Advanced Functional Materials* **2020**, *30*, 2000712.
53. Wandelt, K. *Encyclopedia of interfacial chemistry: surface science and electrochemistry*; Elsevier: 2018.
54. Tee, S.Y.; Win, K.Y.; Goh, S.S.; Teng, C.P.; Tang, K.Y.; Regulacio, M.D.; Li, Z.; Ye, E. Introduction to Photothermal Nanomaterials. **2022**.
55. Vélez-Cordero, J.R.; Hernandez-Cordero, J. Heat generation and conduction in PDMS-carbon nanoparticle membranes irradiated with optical fibers. *International Journal of Thermal Sciences* **2015**, *96*, 12-22.
56. Ye, L.; Cao, Z.; Liu, X.; Cui, Z.; Li, Z.; Liang, Y.; Zhu, S.; Wu, S. Noble metal-based nanomaterials as antibacterial agents. *Journal of Alloys and Compounds* **2022**, 164091.
57. Vines, J.B.; Yoon, J.-H.; Ryu, N.-E.; Lim, D.-J.; Park, H. Gold nanoparticles for photothermal cancer therapy. *Frontiers in chemistry* **2019**, *7*, 167.
58. Hu, M.; Chen, J.; Li, Z.-Y.; Au, L.; Hartland, G.V.; Li, X.; Marquez, M.; Xia, Y. Gold nanostructures: engineering their plasmonic properties for biomedical applications. *Chemical Society Reviews* **2006**, *35*, 1084-1094.
59. Link, S.; El-Sayed, M.A. Size and temperature dependence of the plasmon absorption of colloidal gold nanoparticles. *The Journal of Physical Chemistry B* **1999**, *103*, 4212-4217.
60. Zharov, V.P.; Mercer, K.E.; Galitovskaya, E.N.; Smeltzer, M.S. Photothermal nanotherapeutics and nanodiagnostics for selective killing of bacteria targeted with gold nanoparticles. *Biophysical journal* **2006**, *90*, 619-627.
61. Pihl, M.; Bruzell, E.; Andersson, M. Bacterial biofilm elimination using gold nanorod localised surface plasmon resonance generated heat. *Materials Science and Engineering: C* **2017**, *80*, 54-58.

Preprints (www.preprints.org) | NOT PEER-REVIEWED | Posted: 16 May 2023 doi:10.20944/preprints202305.1106.v1

62. Guan, G.; Win, K.Y.; Yao, X.; Yang, W.; Han, M.Y. Plasmonically modulated gold nanostructures for photothermal ablation of bacteria. *Advanced Healthcare Materials* **2021**, *10*, 2001158.
63. Feng, Y.; Liu, L.; Zhang, J.; Aslan, H.; Dong, M. Photoactive antimicrobial nanomaterials. *Journal of Materials Chemistry B* **2017**, *5*, 8631-8652.
64. Yougbaré, S.; Chou, H.-L.; Yang, C.-H.; Krisnawati, D.I.; Jazidie, A.; Nuh, M.; Kuo, T.-R. Facet-dependent gold nanocrystals for effective photothermal killing of bacteria. *Journal of Hazardous Materials* **2021**, *407*, 124617.
65. Link, S.; Wang, Z.L.; El-Sayed, M.A. How does a gold nanorod melt? *The Journal of Physical Chemistry B* **2000**, *104*, 7867-7870.
66. Yan, J.; Zhu, D.; Xie, J.; Shao, Y.; Xiao, W. Light tailoring of internal atomic structure of gold nanorods. *Small* **2020**, *16*, 2001101.
67. Liao, Z.; Zhang, W.; Qiao, Z.; Luo, J.; Erpuding, A.; Niwaer, A.; Meng, X.; Wang, H.; Li, X.; Zuo, F. Dopamine-assisted one-pot synthesis of gold nanoworms and their application as photothermal agents. *Journal of colloid and interface science* **2020**, *562*, 81-90.
68. Hu, D.; Li, H.; Wang, B.; Ye, Z.; Lei, W.; Jia, F.; Jin, Q.; Ren, K.-F.; Ji, J. Surface-adaptive gold nanoparticles with effective adherence and enhanced photothermal ablation of methicillin-resistant Staphylococcus aureus biofilm. *ACS nano* **2017**, *11*, 9330-9339.
69. Qiao, Z.; Yao, Y.; Song, S.; Yin, M.; Yang, M.; Yan, D.; Yang, L.; Luo, J. Gold nanorods with surface charge-switchable activities for enhanced photothermal killing of bacteria and eradication of biofilm. *Journal of materials chemistry B* **2020**, *8*, 3138-3149.
70. Mahmoud, N.N.; Alkilany, A.M.; Khalil, E.A.; Al-Bakri, A.G. Nano-photothermal ablation effect of hydrophilic and hydrophobic functionalized gold nanorods on Staphylococcus aureus and Propionibacterium acnes. *Scientific Reports* **2018**, *8*, 6881.
71. Zhao, Y.; Guo, Q.; Dai, X.; Wei, X.; Yu, Y.; Chen, X.; Li, C.; Cao, Z.; Zhang, X. A biomimetic non-antibiotic approach to eradicate drug-resistant infections. *Advanced Materials* **2019**, *31*, 1806024.
72. Li, W.; Geng, X.; Liu, D.; Li, Z. Near-infrared light-enhanced protease-conjugated gold nanorods as a photothermal antimicrobial agent for elimination of exotoxin and biofilms. *International Journal of Nanomedicine* **2019**, 8047-8058.
73. Sankari, S.S.; Dahms, H.-U.; Tsai, M.-F.; Lo, Y.-L.; Wang, L.-F. Comparative study of an antimicrobial peptide and a neuropeptide conjugated with gold nanorods for the targeted photothermal killing of bacteria. *Colloids and Surfaces B: Biointerfaces* **2021**, *208*, 112117.
74. Merkl, P.; Zhou, S.; Zaganiaris, A.; Shahata, M.; Eleftheraki, A.; Thersleff, T.; Sotiriou, G.A. Plasmonic coupling in silver nanoparticle aggregates and their polymer composite films for near-infrared photothermal biofilm eradication. *ACS Applied Nano Materials* **2021**, *4*, 5330-5339.
75. Liu, Y.; Li, F.; Guo, Z.; Xiao, Y.; Zhang, Y.; Sun, X.; Zhe, T.; Cao, Y.; Wang, L.; Lu, Q. Silver nanoparticle-embedded hydrogel as a photothermal platform for combating bacterial infections. *Chemical Engineering Journal* **2020**, *382*, 122990.
76. Zhang, H.; Tan, J.; Yang, X.; Ma, Y.; Zou, H.; Wang, Y.; Zhang, P.; Zheng, Y. Size-Tunable Yolk–Shell Gold–Silver Nanostructures for Photothermal Treatment of Multidrug-Resistant Bacteria. *ACS Applied Nano Materials* **2022**, *5*, 10818-10828.
77. Deng, F.; Wu, P.; Qian, G.; Shuai, Y.; Zhang, L.; Peng, S.; Shuai, C.; Wang, G. Silver-decorated black phosphorus: a synergistic antibacterial strategy. *Nanotechnology* **2022**, *33*, 245708.
78. Zhang, H.; Yu, S.; Wu, S.; Xu, M.; Gao, T.; Wu, Q.; Xu, H.; Liu, Y. Rational design of silver NPs-incorporated quaternized chitin nanomicelle with combinational antibacterial capability for infected wound healing. *International Journal of Biological Macromolecules* **2023**, *224*, 1206-1216.
79. Bai, Q.; Liang, M.; Wu, W.; Zhang, C.; Li, X.; Liu, M.; Yang, D.; Yu, W.W.; Hu, Q.; Wang, L. Plasmonic nanozyme of graphdiyne nanowalls wrapped hollow copper sulfide nanocubes for rapid bacteria-killing. *Advanced Functional Materials* **2022**, *32*, 2112683.
80. Wang, X.; Shi, Q.; Zha, Z.; Zhu, D.; Zheng, L.; Shi, L.; Wei, X.; Lian, L.; Wu, K.; Cheng, L. Copper single-atom catalysts with photothermal performance and enhanced nanozyme activity for bacteria-infected wound therapy. *Bioactive materials* **2021**, *6*, 4389-4401.
81. Chen, Y.; Chen, Z.; Yang, D.; Zhu, L.; Liang, Z.; Pang, Y.; Zhou, L. Novel Microbial Palladium Nanoparticles with a High Photothermal Effect for Antibacterial Applications. *ACS omega* **2022**.
82. Li, W.; Fan, Y.; Lin, J.; Yu, P.; Wang, Z.; Ning, C. Near-Infrared Light-Activatable Bismuth-Based Nanomaterials for Antibacterial and Antitumor Treatment. *Advanced Therapeutics* **2022**, *5*, 2200027.
83. Nudelman, R.; Gavriely, S.; Bychenko, D.; Barzilay, M.; Gulakhmedova, T.; Gazit, E.; Richter, S. Bio-assisted synthesis of bimetallic nanoparticles featuring antibacterial and photothermal properties for the removal of biofilms. *Journal of Nanobiotechnology* **2021**, *19*, 1-10.
84. Wang, Z.; Peng, Y.; Zhou, Y.; Zhang, S.; Tan, J.; Li, H.; He, D.; Deng, L. Pd-Cu nanoalloy for dual stimuli-responsive chemo-photothermal therapy against pathogenic biofilm bacteria. *Acta Biomaterialia* **2022**, *137*, 276-289.

Preprints (www.preprints.org) | NOT PEER-REVIEWED | Posted: 16 May 2023 doi:10.20944/preprints202305.1106.v1

85. Mo, S.; Song, Y.; Lin, M.; Wang, J.; Zhang, Z.; Sun, J.; Guo, D.; Liu, L. Near-infrared responsive sulfur vacancy-rich CuS nanosheets for efficient antibacterial activity via synergistic photothermal and photodynamic pathways. *Journal of Colloid and Interface Science* **2022**, *608*, 2896-2906.
86. Zhang, Z.; Wen, J.; Zhang, J.; Guo, D.; Zhang, Q. Vacancy-Modulated of CuS for Highly Antibacterial Efficiency via Photothermal/Photodynamic Synergetic Therapy. *Advanced Healthcare Materials* **2023**, *12*, 2201746.
87. Chen, J.; Qi, C.; Zhang, Y.; Zhang, Q.; Tu, J. Photothermal/lysozyme-catalyzed hydrolysis dual-modality therapy via halloysite nanotube-based platform for effective bacterial eradication. *International Journal of Biological Macromolecules* **2023**, 124530.
88. Mo, S.; Zhao, Y.; Wen, J.; Sun, J.; Zhang, Z.; Yu, Q.; Wang, G.; Chen, X.; Liu, M. Efficient photothermal and photodynamic synergistic antibacterial therapy of Cu7S4 nanosheets regulated by facet engineering. *Journal of Hazardous Materials* **2022**, *432*, 128662.
89. Wu, G.; Wu, Z.; Liu, L.; Cui, W.; Du, D.; Xue, Y. NIR light responsive MoS2 nanomaterials for rapid sterilization: Optimum photothermal effect via sulfur vacancy modulation. *Chemical Engineering Journal* **2022**, *427*, 132007.
90. Wang, C.; Li, J.; Liu, X.; Cui, Z.; Chen, D.-F.; Li, Z.; Liang, Y.; Zhu, S.; Wu, S. The rapid photoresponsive bacteria-killing of Cu-doped MoS 2. *Biomaterials Science* **2020**, *8*, 4216-4224.
91. Wang, X.; Fan, L.; Cheng, L.; Sun, Y.; Wang, X.; Zhong, X.; Shi, Q.; Gong, F.; Yang, Y.; Ma, Y. Biodegradable nickel disulfide nanozymes with GSH-depleting function for high-efficiency photothermal-catalytic antibacterial therapy. *Iscience* **2020**, *23*, 101281.
92. Wang, X.-M.; Huang, L.; Wang, Y.-J.; Xuan, L.; Li, W.-W.; Tian, L.-J. Highly efficient near-infrared photothermal antibacterial membrane with incorporated biogenic CuSe nanoparticles. *Chemical Engineering Journal* **2021**, *405*, 126711.
93. Kim, J.; Yun, H.; Ri, K.; Sun, J.; Kim, H.; Liu, L. NIR-driven SnSe particles for rapid and effective bacteria sterilization. *Journal of Environmental Chemical Engineering* **2023**, *11*, 109109.
94. Guo, J.; Wei, W.; Zhao, Y.; Dai, H. Iron oxide nanoparticles with photothermal performance and enhanced nanozyme activity for bacteria-infected wound therapy. *Regenerative Biomaterials* **2022**, *9*.
95. Lv, X.; Fang, Z.; Sun, Y.; Yang, Y.; Wang, X.; Chen, Y.; Qin, Y.; Li, N.; Li, C.; Xu, J. Interfacial preparation of multi-branched magneto-plasmonic Fe3O4@ Au core@ shell nanocomposites as efficient photothermal agents for antibacterial application. *Journal of Alloys and Compounds* **2023**, *932*, 167712.
96. Hao, S.; Han, H.; Yang, Z.; Chen, M.; Jiang, Y.; Lu, G.; Dong, L.; Wen, H.; Li, H.; Liu, J. Recent advancements on photothermal conversion and antibacterial applications over MXenes-based materials. *Nano-Micro Letters* **2022**, *14*, 178.
97. Rasool, K.; Helal, M.; Ali, A.; Ren, C.E.; Gogotsi, Y.; Mahmoud, K.A. Antibacterial activity of Ti3C2T x MXene. *ACS nano* **2016**, *10*, 3674-3684.
98. Zhang, D.; Huang, L.; Sun, D.-W.; Pu, H.; Wei, Q. Bio-interface engineering of MXene nanosheets with immobilized lysozyme for light-enhanced enzymatic inactivation of methicillin-resistant Staphylococcus aureus. *Chemical Engineering Journal* **2023**, *452*, 139078.
99. Zheng, Y.; Yan, Y.; Lin, L.; He, Q.; Hu, H.; Luo, R.; Xian, D.; Wu, J.; Shi, Y.; Zeng, F. Titanium carbide MXene-based hybrid hydrogel for chemo-photothermal combinational treatment of localized bacterial infection. *Acta Biomaterialia* **2022**, *142*, 113-123.
100. Li, J.; Li, Z.; Liu, X.; Li, C.; Zheng, Y.; Yeung, K.W.K.; Cui, Z.; Liang, Y.; Zhu, S.; Hu, W. Interfacial engineering of Bi2S3/Ti3C2T x MXene based on work function for rapid photo-excited bacteria-killing. *Nature Communications* **2021**, *12*, 1224.
101. Naskar, A.; Kim, K.-s. Black phosphorus nanomaterials as multi-potent and emerging platforms against bacterial infections. *Microbial pathogenesis* **2019**, *137*, 103800.
102. Choi, J.R.; Yong, K.W.; Choi, J.Y.; Nilghaz, A.; Lin, Y.; Xu, J.; Lu, X. Black phosphorus and its biomedical applications. *Theranostics* **2018**, *8*, 1005.
103. Guo, T.; Zhuang, S.; Qiu, H.; Guo, Y.; Wang, L.; Jin, G.; Lin, W.; Huang, G.; Yang, H. Black phosphorus nanosheets for killing bacteria through nanoknife effect. *Particle & Particle Systems Characterization* **2020**, *37*, 2000169.
104. Shi, Z.; Ren, X.; Qiao, H.; Cao, R.; Zhang, Y.; Qi, X.; Zhang, H. Recent insights into the robustness of two-dimensional black phosphorous in optoelectronic applications. *Journal of Photochemistry and Photobiology C: Photochemistry Reviews* **2020**, *43*, 100354.
105. Aksoy, I.; Kucukkececi, H.; Sevgi, F.; Metin, O.; Hatay Patir, I. Photothermal antibacterial and antibiofilm activity of black phosphorus/gold nanocomposites against pathogenic bacteria. *ACS applied materials & interfaces* **2020**, *12*, 26822-26831.
106. Zhang, P.; Sun, B.; Wu, F.; Zhang, Q.; Chu, X.; Ge, M.; Zhou, N.; Shen, J. Wound healing acceleration by antibacterial biodegradable black phosphorus nanosheets loaded with cationic carbon dots. *Journal of Materials Science* **2021**, *56*, 6411-6426.

Preprints (www.preprints.org) | NOT PEER-REVIEWED | Posted: 16 May 2023 doi:10.20944/preprints202305.1106.v1

107. Naskar, A.; Cho, H.; Kim, K.-s. Black phosphorus-based CuS nanoplatform: Near-infrared-responsive and reactive oxygen species-generating agent against environmental bacterial pathogens. *Journal of Environmental Chemical Engineering* **2022**, *10*, 108226.
108. Zhao, Y.; Liu, Y.; Tian, C.; Liu, Z.; Wu, K.; Zhang, C.; Han, X. Construction of antibacterial photothermal PCL/AgNPs/BP nanofibers for infected wound healing. *Materials & Design* **2023**, *226*, 111670.
109. Çekceoğlu, İ.A.; Eroglu, Z.; Küçükkeçeci, H.; Sevgi, F.; Ersoz, M.; Patir, I.H.; Metin, Ö. A NIR-light-driven Black Phosphorus Based Nanocomposite for Combating Bacteria. *ChemistrySelect* **2022**, *7*, e202104137.
110. Zhang, Q.; Liu, X.; Tan, L.; Cui, Z.; Li, Z.; Liang, Y.; Zhu, S.; Yeung, K.; Zheng, Y.; Wu, S. An UV to NIR-driven platform based on red phosphorus/graphene oxide film for rapid microbial inactivation. *Chemical Engineering Journal* **2020**, *383*, 123088.
111. Lv, J.; Qi, Y.; Tian, Y.; Wang, G.; Shi, L.; Ning, G.; Ye, J. Functionalized boron nanosheets with near-infrared-triggered photothermal and nitric oxide release activities for efficient antibacterial treatment and wound healing promotion. *Biomaterials Science* **2022**, *10*, 3747-3756.
112. Liu, B.; Su, Y.; Wu, S.; Shen, J. Local photothermal/photodynamic synergistic antibacterial therapy based on two-dimensional BP@ CQDs triggered by single NIR light source. *Photodiagnosis and Photodynamic Therapy* **2022**, *39*, 102905.
113. Chen, Y.; Gao, Y.; Chen, Y.; Liu, L.; Mo, A.; Peng, Q. Nanomaterials-based photothermal therapy and its potentials in antibacterial treatment. *Journal of Controlled Release* **2020**, *328*, 251-262.
114. Saleem, J.; Wang, L.; Chen, C. Carbon-based nanomaterials for cancer therapy via targeting tumor microenvironment. *Advanced healthcare materials* **2018**, *7*, 1800525.
115. Khan, A.A.P.; Khan, A.; Rahman, M.M.; Asiri, A.M.; Oves, M. Lead sensors development and antimicrobial activities based on graphene oxide/carbon nanotube/poly (O-toluidine) nanocomposite. *International journal of biological macromolecules* **2016**, *89*, 198-205.
116. Akhavan, O.; Ghaderi, E. Toxicity of graphene and graphene oxide nanowalls against bacteria. *ACS nano* **2010**, *4*, 5731-5736.
117. Kang, S.; Herzberg, M.; Rodrigues, D.F.; Elimelech, M. Antibacterial effects of carbon nanotubes: size does matter! *Langmuir* **2008**, *24*, 6409-6413.
118. Catanio, A.T.; Bergmann, E.V.; Kimura, N.M.; Petrucci, T.; Freitas, C.F.; Herculano, L.S.; Malacarne, L.C.; Astrath, N.G. Spectroscopic and photothermal characterization of graphene quantum dots for antimicrobial applications. *Journal of Applied Physics* **2022**, *131*, 155102.
119. Qie, X.; Zan, M.; Gui, P.; Chen, H.; Wang, J.; Lin, K.; Mei, Q.; Ge, M.; Zhang, Z.; Tang, Y. Design, synthesis, and application of carbon dots with synergistic antibacterial activity. *Frontiers in Bioengineering and Biotechnology* **2022**, *10*.
120. Feng, Y.; Chen, Q.; Yin, Q.; Pan, G.; Tu, Z.; Liu, L. Reduced graphene oxide functionalized with gold nanostar nanocomposites for synergistically killing bacteria through intrinsic antimicrobial activity and photothermal ablation. *ACS Applied Bio Materials* **2019**, *2*, 747-756.
121. Oruc, B.; Unal, H. Fluorophore-decorated carbon nanotubes with enhanced photothermal activity as antimicrobial nanomaterials. *ACS Omega* **2019**, *4*, 5556-5564.
122. Tan, S.; Wu, X.; Xing, Y.; Lilak, S.; Wu, M.; Zhao, J.X. Enhanced synergetic antibacterial activity by a reduce graphene oxide/Ag nanocomposite through the photothermal effect. *Colloids and Surfaces B: Biointerfaces* **2020**, *185*, 110616.
123. Chen, Y.; Wu, W.; Xu, Z.; Jiang, C.; Han, S.; Ruan, J.; Wang, Y. Photothermal-assisted antibacterial application of graphene oxide-Ag nanocomposites against clinically isolated multi-drug resistant Escherichia coli. *Royal Society Open Science* **2020**, *7*, 192019.
124. Yang, Y.; Yin, H.; Li, H.; Zou, Q.; Zhang, Z.; Pei, W.; Luo, L.; Huo, Y.; Li, H. Synergistic photocatalytic-photothermal contribution to antibacterial activity in BiOI-graphene oxide nanocomposites. *ACS Applied Bio Materials* **2018**, *1*, 2141-2152.
125. Lv, Y.-k.; Mei, L.; Zhang, L.-x.; Yang, D.-h.; Yin, Z.-y. Multifunctional graphene-based nanocomposites for simultaneous enhanced photocatalytic degradation and photothermal antibacterial activity by visible light. *Environmental Science and Pollution Research* **2021**, *28*, 49880-49888.
126. Lin, F.; Duan, Q.-Y.; Wu, F.-G. Conjugated polymer-based photothermal therapy for killing microorganisms. *ACS Applied Polymer Materials* **2020**, *2*, 4331-4344.
127. Pham, T.-T.D.; Phan, L.M.T.; Cho, S.; Park, J. Enhancement approaches for photothermal conversion of donor–acceptor conjugated polymer for photothermal therapy: a review. *Science and Technology of Advanced Materials* **2022**, *23*, 707-734.
128. Zhou, S.; Wang, Z.; Wang, Y.; Feng, L. Near-infrared light-triggered synergistic phototherapy for antimicrobial therapy. *ACS Applied Bio Materials* **2020**, *3*, 1730-1737.
129. Ko, Y.; Kim, J.; Jeong, H.Y.; Kwon, G.; Kim, D.; Ku, M.; Yang, J.; Yamauchi, Y.; Kim, H.-Y.; Lee, C. Antibacterial poly (3, 4-ethylenedioxythiophene): poly (styrene-sulfonate)/agarose nanocomposite hydrogels with thermo-processability and self-healing. *Carbohydrate polymers* **2019**, *203*, 26-34.

Preprints (www.preprints.org) | NOT PEER-REVIEWED | Posted: 16 May 2023 doi:10.20944/preprints202305.1106.v1

130. Wang, X.; Zhu, L.; Gu, Z.; Dai, L. Carbon nanomaterials for phototherapy. *Nanophotonics* **2022**, *11*, 4955-4976.
131. Fan, X.-L.; Li, H.-Y.; Ye, W.-Y.; Zhao, M.-Q.; Huang, D.-n.; Fang, Y.; Zhou, B.-Q.; Ren, K.-F.; Ji, J.; Fu, G.-S. Magainin-modified polydopamine nanoparticles for photothermal killing of bacteria at low temperature. *Colloids and Surfaces B: Biointerfaces* **2019**, *183*, 110423.
132. Jia, X.; Ahmad, I.; Yang, R.; Wang, C. Versatile graphene-based photothermal nanocomposites for effectively capturing and killing bacteria, and for destroying bacterial biofilms. *Journal of Materials Chemistry B* **2017**, *5*, 2459-2467.
133. Korupalli, C.; Huang, C.-C.; Lin, W.-C.; Pan, W.-Y.; Lin, P.-Y.; Wan, W.-L.; Li, M.-J.; Chang, Y.; Sung, H.-W. Acidity-triggered charge-convertible nanoparticles that can cause bacterium-specific aggregation in situ to enhance photothermal ablation of focal infection. *Biomaterials* **2017**, *116*, 1-9.
134. Wang, Y.; Li, S.; Liu, L.; Feng, L. Photothermal-responsive conjugated polymer nanoparticles for the rapid and effective killing of bacteria. *ACS Applied Bio Materials* **2018**, *1*, 27-32.
135. Mohajer, F.; Ziarani, G.M.; Badiei, A.; Iravani, S.; Varma, R.S. Recent advances in covalent organic frameworks (COFs) for wound healing and antimicrobial applications. *RSC advances* **2023**, *13*, 8136-8152.
136. Li, P.; Li, B.; Wang, C.; Zhao, X.; Zheng, Y.; Wu, S.; Shen, J.; Zhang, Y.; Liu, X. In situ fabrication of co-coordinated TCPP-Cur donor-acceptor-type covalent organic framework-like photocatalytic hydrogel for rapid therapy of bacteria-infected wounds. *Composites Part B: Engineering* **2023**, 110506.
137. Schlachter, A.; Asselin, P.; Harvey, P.D. Porphyrin-containing MOFs and COFs as heterogeneous photosensitizers for singlet oxygen-based antimicrobial nanodevices. *ACS Applied Materials & Interfaces* **2021**, *13*, 26651-26672.
138. Zhang, L.; Wang, S.; Zhou, Y.; Wang, C.; Zhang, X.Z.; Deng, H. Covalent organic frameworks as favorable constructs for photodynamic therapy. *Angewandte Chemie International Edition* **2019**, *58*, 14213-14218.
139. Sun, B.; Ye, Z.; Zhang, M.; Song, Q.; Chu, X.; Gao, S.; Zhang, Q.; Jiang, C.; Zhou, N.; Yao, C. Light-activated biodegradable covalent organic framework-integrated heterojunction for photodynamic, photothermal, and gaseous therapy of chronic wound infection. *ACS Applied Materials & Interfaces* **2021**, *13*, 42396-42410.
140. Yang, G.-P.; Meng, X.-L.; Xiao, S.-J.; Zheng, Q.-Q.; Tan, Q.-G.; Liang, R.-P.; Zhang, L.; Zhang, P.; Qiu, J.-D. Construction of D–A-Conjugated Covalent Organic Frameworks with Enhanced Photodynamic, Photothermal, and Nanozymatic Activities for Efficient Bacterial Inhibition. *ACS Applied Materials & Interfaces* **2022**, *14*, 28289-28300.
141. Yang, F.; Feng, Y.; Fan, X.; Zhang, M.; Wang, C.; Zhao, W.; Zhao, C. Biocompatible graphene-based nanoagent with NIR and magnetism dual-responses for effective bacterial killing and removal. *Colloids and Surfaces B: Biointerfaces* **2019**, *173*, 266-275.
142. Yang, Y.; Ma, L.; Cheng, C.; Deng, Y.; Huang, J.; Fan, X.; Nie, C.; Zhao, W.; Zhao, C. Nonchemotherapic and robust dual-responsive nanoagents with on-demand bacterial trapping, ablation, and release for efficient wound disinfection. *Advanced Functional Materials* **2018**, *28*, 1705708.
143. Zhang, Y.; Zhou, S.; Chong, K.C.; Wang, S.; Liu, B. Near-infrared light-induced shape memory, self-healable and anti-bacterial elastomers prepared by incorporation of a diketopyrrolopyrrole-based conjugated polymer. *Materials Chemistry Frontiers* **2019**, *3*, 836-841.
144. Zhang, H.; Liang, Y.; Zhao, H.; Qi, R.; Chen, Z.; Yuan, H.; Liang, H.; Wang, L. Dual-Mode Antibacterial Conjugated Polymer Nanoparticles for Photothermal and Photodynamic Therapy. *Macromolecular Bioscience* **2020**, *20*, 1900301.
145. Han, L.; Li, P.; Tang, P.; Wang, X.; Zhou, T.; Wang, K.; Ren, F.; Guo, T.; Lu, X. Mussel-inspired cryogels for promoting wound regeneration through photobiostimulation, modulating inflammatory responses and suppressing bacterial invasion. *Nanoscale* **2019**, *11*, 15846-15861.
146. Wang, X.; Sun, X.; Bu, T.; Wang, Q.; Jia, P.; Dong, M.; Wang, L. In situ fabrication of metal-organic framework derived hybrid nanozymes for enhanced nanozyme-photothermal therapy of bacteria-infected wounds. *Composites Part B: Engineering* **2022**, *229*, 109465.
147. Xu, X.; Liu, Y.; Fu, W.; Yao, M.; Ding, Z.; Xuan, J.; Li, D.; Wang, S.; Xia, Y.; Cao, M. Poly (N-isopropylacrylamide)-based thermoresponsive composite hydrogels for biomedical applications. *Polymers* **2020**, *12*, 580.
148. Liu, Z.; Zhao, X.; Yu, B.; Zhao, N.; Zhang, C.; Xu, F.-J. Rough carbon–iron oxide nanohybrids for near-infrared-II light-responsive synergistic antibacterial therapy. *ACS nano* **2021**, *15*, 7482-7490.
149. Xu, Y.; Wang, K.; Zhao, S.; Xiong, Q.; Liu, G.; Li, Y.; Fang, Q.; Gong, X.; Xuan, S. Rough surface NiFe2O4@ Au/Polydopamine with a magnetic field enhanced photothermal antibacterial effect. *Chemical Engineering Journal* **2022**, *437*, 135282.
150. Zheng, H.; Li, H.; Deng, H.; Fang, W.; Huang, X.; Qiao, J.; Tong, Y. Near infrared light-responsive and drug-loaded black phosphorus nanosheets for antibacterial applications. *Colloids and Surfaces B: Biointerfaces* **2022**, *214*, 112433.

Preprints (www.preprints.org) | NOT PEER-REVIEWED | Posted: 16 May 2023 doi:10.20944/preprints202305.1106.v1

151. Yan, H.; Zhang, B.; Zhang, Y.; Su, R.; Li, P.; Su, W. Fluorescent carbon dot–curcumin nanocomposites for remarkable antibacterial activity with synergistic photodynamic and photothermal abilities. *ACS Applied Bio Materials* **2021**, *4*, 6703-6718.
152. Moorcroft, S.C.; Roach, L.; Jayne, D.G.; Ong, Z.Y.; Evans, S.D. Nanoparticle-loaded hydrogel for the light-activated release and photothermal enhancement of antimicrobial peptides. *ACS applied materials & interfaces* **2020**, *12*, 24544-24554.
153. Dong, X.; Ye, J.; Chen, Y.; Tanziela, T.; Jiang, H.; Wang, X. Intelligent peptide-nanorods against drug-resistant bacterial infection and promote wound healing by mild-temperature photothermal therapy. *Chemical Engineering Journal* **2022**, *432*, 134061.
154. Huang, S.; Xu, S.; Hu, Y.; Zhao, X.; Chang, L.; Chen, Z.; Mei, X. Preparation of NIR-responsive, ROS-generating and antibacterial black phosphorus quantum dots for promoting the MRSA-infected wound healing in diabetic rats. *Acta biomaterialia* **2022**, *137*, 199-217.
155. Cao, W.; Yue, L.; Khan, I.M.; Wang, Z. Polyethylenimine modified MoS2 nanocomposite with high stability and enhanced photothermal antibacterial activity. *Journal of Photochemistry and Photobiology A: Chemistry* **2020**, *401*, 112762.
156. Li, H.; Gong, M.; Xiao, J.; Hai, L.; Luo, Y.; He, L.; Wang, Z.; Deng, L.; He, D. Photothermally activated multifunctional MoS2 bactericidal nanoplatform for combined chemo/photothermal/photodynamic triple-mode therapy of bacterial and biofilm infections. *Chemical Engineering Journal* **2022**, *429*, 132600.
157. Xu, M.; Hu, Y.; Xiao, Y.; Zhang, Y.; Sun, K.; Wu, T.; Lv, N.; Wang, W.; Ding, W.; Li, F. Near-infrared-controlled nanoplatform exploiting photothermal promotion of peroxidase-like and OXD-like activities for potent antibacterial and anti-biofilm therapies. *ACS Applied Materials & Interfaces* **2020**, *12*, 50260-50274.
158. Ziesmer, J.; Larsson, J.V.; Sotiriou, G.A. Hybrid microneedle arrays for antibiotic and near-IR photothermal synergistic antimicrobial effect against Methicillin-Resistant Staphylococcus aureus. *Chemical Engineering Journal* **2023**, *462*, 142127.
159. Gan, Y.; Lin, C.; Zhu, H.; Cheng, X.; Liu, C.; Shi, J. An injectable self-healing CS/PDA–AgNPs hybrid hydrogel for mild and highly-efficient photothermal sterilization. *New Journal of Chemistry* **2022**, *46*, 8043-8052.
160. Prinz Setter, O.; Snoyman, I.; Shalash, G.; Segal, E. Gold Nanorod-Incorporated Halloysite Nanotubes Functionalized with Antibody for Superior Antibacterial Photothermal Treatment. *Pharmaceutics* **2022**, *14*, 2094.
161. Abee, T.; Kovács, Á.T.; Kuipers, O.P.; Van der Veen, S. Biofilm formation and dispersal in Gram-positive bacteria. *Current opinion in biotechnology* **2011**, *22*, 172-179.
162. Flemming, H.-C.; van Hullebusch, E.D.; Neu, T.R.; Nielsen, P.H.; Seviour, T.; Stoodley, P.; Wingender, J.; Wuertz, S. The biofilm matrix: Multitasking in a shared space. *Nature Reviews Microbiology* **2023**, *21*, 70-86.
163. Ikuma, K.; Decho, A.W.; Lau, B.L. When nanoparticles meet biofilms—interactions guiding the environmental fate and accumulation of nanoparticles. *Frontiers in microbiology* **2015**, *6*, 591.
164. Makabenta, J.M.V.; Nabawy, A.; Li, C.-H.; Schmidt-Malan, S.; Patel, R.; Rotello, V.M. Nanomaterial-based therapeutics for antibiotic-resistant bacterial infections. *Nature Reviews Microbiology* **2021**, *19*, 23-36.
165. Qi, Z.; Bharate, P.; Lai, C.-H.; Ziem, B.; Bo¨ttcher, C.; Schulz, A.; Beckert, F.; Hatting, B.; Mu¨lhaupt, R.; Seeberger, P.H. Multivalency at interfaces: supramolecular carbohydrate-functionalized graphene derivatives for bacterial capture, release, and disinfection. *Nano letters* **2015**, *15*, 6051-6057.
166. Teng, W.; Zhang, Z.; Wang, Y.; Ye, Y.; Yinwang, E.; Liu, A.; Zhou, X.; Xu, J.; Zhou, C.; Sun, H. Iodine Immobilized Metal–Organic Framework for NIR-Triggered Antibacterial Therapy on Orthopedic Implants. *Small* **2021**, *17*, 2102315.
167. Donlan, R.M. Biofilm formation: a clinically relevant microbiological process. *Clinical infectious diseases* **2001**, *33*, 1387-1392.
168. Elbourne, A.; Cheeseman, S.; Atkin, P.; Truong, N.P.; Syed, N.; Zavabeti, A.; Mohiuddin, M.; Esrafilzadeh, D.; Cozzolino, D.; McConville, C.F. Antibacterial liquid metals: biofilm treatment via magnetic activation. *ACS nano* **2020**, *14*, 802-817.
169. Sun, J.; Song, L.; Fan, Y.; Tian, L.; Luan, S.; Niu, S.; Ren, L.; Ming, W.; Zhao, J. Synergistic photodynamic and photothermal antibacterial nanocomposite membrane triggered by single NIR light source. *ACS applied materials & interfaces* **2019**, *11*, 26581-26589.
170. Xu, Y.; Cai, Y.; Xia, Y.; Wu, Q.; Li, M.; Guo, N.; Tu, Y.; Yang, B.; Liu, Y. Photothermal nanoagent for anti-inflammation through macrophage repolarization following antibacterial therapy. *European Polymer Journal* **2023**, 111840.
171. Shariati, A.; Hosseini, S.M.; Chegini, Z.; Seifalian, A.; Arabestani, M.R. Graphene-Based Materials for Inhibition of Wound Infection and Accelerating Wound Healing. *Biomedicine & Pharmacotherapy* **2023**, *158*, 114184.
172. Cao, F.; Ju, E.; Zhang, Y.; Wang, Z.; Liu, C.; Li, W.; Huang, Y.; Dong, K.; Ren, J.; Qu, X. An efficient and benign antimicrobial depot based on silver-infused MoS2. *ACS nano* **2017**, *11*, 4651-4659.

Preprints (www.preprints.org) | NOT PEER-REVIEWED | Posted: 16 May 2023 doi:10.20944/preprints202305.1106.v1

173. Chernousova, S.; Epple, M. Silver as antibacterial agent: ion, nanoparticle, and metal. *Angewandte Chemie International Edition* **2013**, *52*, 1636-1653.
174. Liu, M.; He, D.; Yang, T.; Liu, W.; Mao, L.; Zhu, Y.; Wu, J.; Luo, G.; Deng, J. An efficient antimicrobial depot for infectious site-targeted chemo-photothermal therapy. *Journal of nanobiotechnology* **2018**, *16*, 1-20.
175. AshaRani, P.; Low Kah Mun, G.; Hande, M.P.; Valiyaveettil, S. Cytotoxicity and genotoxicity of silver nanoparticles in human cells. *ACS nano* **2009**, *3*, 279-290.
176. Rtimi, S.; Dionysiou, D.D.; Pillai, S.C.; Kiwi, J. Advances in catalytic/photocatalytic bacterial inactivation by nano Ag and Cu coated surfaces and medical devices. *Applied Catalysis B: Environmental* **2019**, *240*, 291-318.
177. Cao, J.; Sun, Q.; Shen, A.-G.; Fan, B.; Hu, J.-M. Nano Au@ Cu2-xS with near-infrared photothermal and peroxidase catalytic activities redefines efficient antibiofilm-oriented root canal therapy. *Chemical Engineering Journal* **2021**, *422*, 130090.
178. Bao, X.; Zheng, S.; Zhang, L.; Shen, A.; Zhang, G.; Liu, S.; Hu, J. Nitric-Oxide-Releasing aza-BODIPY: A New Near-Infrared J-Aggregate with Multiple Antibacterial Modalities. *Angewandte Chemie International Edition* **2022**, *61*, e202207250.
179. Yuan, Z.; Lin, C.; He, Y.; Tao, B.; Chen, M.; Zhang, J.; Liu, P.; Cai, K. Near-infrared light-triggered nitric-oxide-enhanced photodynamic therapy and low-temperature photothermal therapy for biofilm elimination. *ACS nano* **2020**, *14*, 3546-3562.
180. Yu, X.; Zhao, J.; Fan, D. A dissolving microneedle patch for antibiotic/enzymolysis/photothermal triple therapy against bacteria and their biofilms. *Chemical Engineering Journal* **2022**, *437*, 135475.
181. Yuan, Z.; Lin, C.; Dai, L.; He, Y.; Hu, J.; Xu, K.; Tao, B.; Liu, P.; Cai, K. Near-infrared light-activatable dual-action nanoparticle combats the established biofilms of methicillin-resistant Staphylococcus aureus and its accompanying inflammation. *Small* **2021**, *17*, 2007522.
182. Li, Y.; Liu, X.; Li, B.; Zheng, Y.; Han, Y.; Chen, D.-f.; Yeung, K.W.K.; Cui, Z.; Liang, Y.; Li, Z. Near-infrared light triggered phototherapy and immunotherapy for elimination of methicillin-resistant Staphylococcus aureus biofilm infection on bone implant. *ACS nano* **2020**, *14*, 8157-8170.
183. Zhao, Y.-Q.; Sun, Y.; Zhang, Y.; Ding, X.; Zhao, N.; Yu, B.; Zhao, H.; Duan, S.; Xu, F.-J. Well-defined gold nanorod/polymer hybrid coating with inherent antifouling and photothermal bactericidal properties for treating an infected hernia. *Acs Nano* **2020**, *14*, 2265-2275.
184. Pircalabioru, G.G.; Chifiriuc, M.-C. Nanoparticulate drug-delivery systems for fighting microbial biofilms: From bench to bedside. *Future Microbiology* **2020**, *15*, 679-698.
185. Cao, Z.; Luo, Y.; Li, Z.; Tan, L.; Liu, X.; Li, C.; Zheng, Y.; Cui, Z.; Yeung, K.W.K.; Liang, Y. Antibacterial hybrid hydrogels. *Macromolecular Bioscience* **2021**, *21*, 2000252.
186. Xu, M.; Li, L.; Hu, Q. The recent progress in photothermal-triggered bacterial eradication. *Biomaterials Science* **2021**, *9*, 1995-2008.
187. Xie, C.; Zhang, Q.; Li, Z.; Ge, S.; Ma, B. Sustained and microenvironment-accelerated release of minocycline from alginate injectable hydrogel for bacteria-infected wound healing. *Polymers* **2022**, *14*, 1816.
188. Guo, C.; Wu, Y.; Li, W.; Wang, Y.; Kong, Q. Development of a microenvironment-responsive hydrogel promoting chronically infected diabetic wound healing through sequential hemostatic, antibacterial, and angiogenic activities. *ACS Applied Materials & Interfaces* **2022**, *14*, 30480-30492.
189. Zhu, Y.; Matsumura, Y.; Velayutham, M.; Foley, L.M.; Hitchens, T.K.; Wagner, W.R. Reactive oxygen species scavenging with a biodegradable, thermally responsive hydrogel compatible with soft tissue injection. *Biomaterials* **2018**, *177*, 98-112.
190. Yan, X.; Yang, J.; Wu, J.; Su, H.; Sun, G.; Ni, Y.; Sun, W. Antibacterial carbon dots/iron oxychloride nanoplatform for chemodynamic and photothermal therapy. *Colloid and Interface Science Communications* **2021**, *45*, 100552.
191. Lin, L.S.; Song, J.; Song, L.; Ke, K.; Liu, Y.; Zhou, Z.; Shen, Z.; Li, J.; Yang, Z.; Tang, W. Simultaneous Fenton-like ion delivery and glutathione depletion by MnO2-based nanoagent to enhance chemodynamic therapy. *Angewandte Chemie* **2018**, *130*, 4996-5000.
192. Sai, D.L.; Lee, J.; Nguyen, D.L.; Kim, Y.-P. Tailoring photosensitive ROS for advanced photodynamic therapy. *Experimental & Molecular Medicine* **2021**, *53*, 495-504.
193. Han, H.; Xu, X.; Kan, H.; Tang, Y.; Liu, C.; Wen, H.; Wu, L.; Jiang, Y.; Wang, Z.; Liu, J. Synergistic photodynamic/photothermal bacterial inactivation over heterogeneous quaternized chitosan/silver/cobalt phosphide nanocomposites. *Journal of Colloid and Interface Science* **2022**, *616*, 304-315.
194. Dai, X.; Zhao, Y.; Yu, Y.; Chen, X.; Wei, X.; Zhang, X.; Li, C. All-in-one NIR-activated nanoplatforms for enhanced bacterial biofilm eradication. *Nanoscale* **2018**, *10*, 18520-18530.
195. Syama, S.; Mohanan, P. Comprehensive application of graphene: emphasis on biomedical concerns. *Nano-micro letters* **2019**, *11*, 1-31.
196. Chu, X.; Zhang, P.; Wang, Y.; Sun, B.; Liu, Y.; Zhang, Q.; Feng, W.; Li, Z.; Li, K.; Zhou, N. Near-infrared carbon dot-based platform for bioimaging and photothermal/photodynamic/quaternary ammonium triple synergistic sterilization triggered by single NIR light source. *Carbon* **2021**, *176*, 126-138.

Preprints (www.preprints.org) | NOT PEER-REVIEWED | Posted: 16 May 2023 doi:10.20944/preprints202305.1106.v1

197. Zhang, Y.; Yan, H.; Tang, J.; Li, P.; Su, R.; Zhong, H.; Su, W. Dual-mode antibacterial core-shell gold nanorod@ mesoporous-silica/curcumin nanocomplexes for efficient photothermal and photodynamic therapy. *Journal of Photochemistry and Photobiology A: Chemistry* **2022**, *425*, 113722.
198. Dong, M.; Sun, X.; Bu, T.; Zhang, H.; Wang, J.; He, K.; Li, L.; Li, Z.; Wang, L. 3D/2D TMSs/TiO2 nanofibers heterojunctions for photodynamic-photothermal and oxidase-like synergistic antibacterial therapy co-driven by VIS and NIR biowindows. *Composites Part B: Engineering* **2022**, *230*, 109498.
199. Xu, Z.; Qiu, Z.; Liu, Q.; Huang, Y.; Li, D.; Shen, X.; Fan, K.; Xi, J.; Gu, Y.; Tang, Y. Converting organosulfur compounds to inorganic polysulfides against resistant bacterial infections. *Nature communications* **2018**, *9*, 3713.
200. Mao, C.; Xiang, Y.; Liu, X.; Zheng, Y.; Yeung, K.W.K.; Cui, Z.; Yang, X.; Li, Z.; Liang, Y.; Zhu, S. Local photothermal/photodynamic synergistic therapy by disrupting bacterial membrane to accelerate reactive oxygen species permeation and protein leakage. *ACS applied materials & interfaces* **2019**, *11*, 17902-17914.
201. Chang, R.; Zhao, D.; Zhang, C.; Liu, K.; He, Y.; Guan, F.; Yao, M. Nanocomposite multifunctional hyaluronic acid hydrogel with photothermal antibacterial and antioxidant properties for infected wound healing. *International Journal of Biological Macromolecules* **2023**, *226*, 870-884.
202. Su, Y.; Zhang, X.; Wei, Y.; Gu, Y.; Xu, H.; Liao, Z.; Zhao, L.; Du, J.; Hu, Y.; Lian, X. Nanocatalytic Hydrogel with Rapid Photodisinfection and Robust Adhesion for Fortified Cutaneous Regeneration. *ACS Applied Materials & Interfaces* **2023**, *15*, 6354-6370.
203. Hu, H.; Wang, H.; Yang, Y.; Xu, J.F.; Zhang, X. A Bacteria-Responsive Porphyrin for Adaptable Photodynamic/Photothermal Therapy. *Angewandte Chemie* **2022**, *134*, e202200799.
204. Lv, R.; Liang, Y.-Q.; Li, Z.-Y.; Zhu, S.-L.; Cui, Z.-D.; Wu, S.-L. Flower-like CuS/graphene oxide with photothermal and enhanced photocatalytic effect for rapid bacteria-killing using visible light. *Rare Metals* **2022**, *41*, 639-649.
205. Rong, F.; Tang, Y.; Wang, T.; Feng, T.; Song, J.; Li, P.; Huang, W. Nitric oxide-releasing polymeric materials for antimicrobial applications: a review. *Antioxidants* **2019**, *8*, 556.
206. Zhao, B.; Wang, H.; Dong, W.; Cheng, S.; Li, H.; Tan, J.; Zhou, J.; He, W.; Li, L.; Zhang, J. A multifunctional platform with single-NIR-laser-triggered photothermal and NO release for synergistic therapy against multidrug-resistant Gram-negative bacteria and their biofilms. *Journal of Nanobiotechnology* **2020**, *18*, 1-25.
207. Yu, S.; Li, G.; Liu, R.; Ma, D.; Xue, W. Dendritic Fe3O4@ poly (dopamine)@ PAMAM nanocomposite as controllable NO-releasing material: a synergistic photothermal and NO antibacterial study. *Advanced Functional Materials* **2018**, *28*, 1707440.
208. Gao, Q.; Zhang, X.; Yin, W.; Ma, D.; Xie, C.; Zheng, L.; Dong, X.; Mei, L.; Yu, J.; Wang, C. Functionalized MoS2 nanovehicle with near-infrared laser-mediated nitric oxide release and photothermal activities for advanced bacteria-infected wound therapy. *Small* **2018**, *14*, 1802290.
209. Liang, Z.; Liu, W.; Wang, Z.; Zheng, P.; Liu, W.; Zhao, J.; Zhong, Y.; Zhang, Y.; Lin, J.; Xue, W. Near-infrared laser-controlled nitric oxide-releasing gold nanostar/hollow polydopamine Janus nanoparticles for synergistic elimination of methicillin-resistant Staphylococcus aureus and wound healing. *Acta Biomaterialia* **2022**, *143*, 428-444.
210. Deng, X.; Liang, S.; Cai, X.; Huang, S.; Cheng, Z.; Shi, Y.; Pang, M.; Ma, P.a.; Lin, J. Yolk–shell structured Au nanostar@ metal–organic framework for synergistic chemo-photothermal therapy in the second near-infrared window. *Nano Letters* **2019**, *19*, 6772-6780.
211. Qing, G.; Zhao, X.; Gong, N.; Chen, J.; Li, X.; Gan, Y.; Wang, Y.; Zhang, Z.; Zhang, Y.; Guo, W. Thermo-responsive triple-function nanotransporter for efficient chemo-photothermal therapy of multidrug-resistant bacterial infection. *Nature communications* **2019**, *10*, 4336.
212. Zou, Z.; Sun, J.; Li, Q.; Pu, Y.; Liu, J.; Sun, R.; Wang, L.; Jiang, T. Vancomycin modified copper sulfide nanoparticles for photokilling of vancomycin-resistant enterococci bacteria. *Colloids and Surfaces B: Biointerfaces* **2020**, *189*, 110875.
213. Yang, N.; Guo, H.; Cao, C.; Wang, X.; Song, X.; Wang, W.; Yang, D.; Xi, L.; Mou, X.; Dong, X. Infection microenvironment-activated nanoparticles for NIR-II photoacoustic imaging-guided photothermal/chemodynamic synergistic anti-infective therapy. *Biomaterials* **2021**, *275*, 120918.
214. Zhu, X.; Chen, X.; Jia, Z.; Huo, D.; Liu, Y.; Liu, J. Cationic chitosan@ Ruthenium dioxide hybrid nanozymes for photothermal therapy enhancing ROS-mediated eradicating multidrug resistant bacterial infection. *Journal of Colloid and Interface Science* **2021**, *603*, 615-632.
215. Lin, X.; Fang, Y.; Hao, Z.; Wu, H.; Zhao, M.; Wang, S.; Liu, Y. Bacteria-Triggered Multifunctional Hydrogel for Localized Chemodynamic and Low-Temperature Photothermal Sterilization. *Small* **2021**, *17*, 2103303.
216. Li, J.; Yi, W.; Luo, Y.; Yang, K.; He, L.; Xu, C.; Deng, L.; He, D. GSH-depleting and H2O2-self-supplying hybrid nanozymes for intensive catalytic antibacterial therapy by photothermal-augmented co-catalysis. *Acta Biomaterialia* **2023**, *155*, 588-600.
217. Guo, N.; Xia, Y.; Duan, Y.; Wu, Q.; Xiao, L.; Shi, Y.; Yang, B.; Liu, Y. Self-enhanced photothermal-chemodynamic antibacterial agents for synergistic anti-infective therapy. *Chinese Chemical Letters* **2023**, *34*, 107542.

Preprints (www.preprints.org) | NOT PEER-REVIEWED | Posted: 16 May 2023 doi:10.20944/preprints202305.1106.v1

218. Luo, X.; Zhang, L.; Luo, Y.; Cai, Z.; Zeng, H.; Wang, T.; Liu, Z.; Chen, Y.; Sheng, X.; Mandlate, A.E.d.G. Charge-Driven Self-Assembled Microspheres Hydrogel Scaffolds for Combined Drug Delivery and Photothermal Therapy of Diabetic Wounds. *Advanced Functional Materials* **2023**, 2214036.
219. Sun, J.; Liu, C.; Wang, Q.; Yang, H.; Gao, X.; Deng, Y.; Yang, W.; He, M. Bimetal-Doped Nanosheet with Phototherapeutic Potential for Clearance of Bacterial Infection. *Materials Letters* **2023**, 133884.
220. Huo, J.; Jia, Q.; Huang, H.; Zhang, J.; Li, P.; Dong, X.; Huang, W. Emerging photothermal-derived multimodal synergistic therapy in combating bacterial infections. *Chemical Society Reviews* **2021**, *50*, 8762-8789.
221. Wang, R.; Liu, Q.; Gao, A.; Tang, N.; Zhang, Q.; Zhang, A.; Cui, D. Recent developments of sonodynamic therapy in antibacterial application. *Nanoscale* **2022**.
222. Bi, X.; Bai, Q.; Liang, M.; Yang, D.; Li, S.; Wang, L.; Liu, J.; Yu, W.W.; Sui, N.; Zhu, Z. Silver peroxide nanoparticles for combined antibacterial sonodynamic and photothermal therapy. *Small* **2022**, *18*, 2104160.
223. He, W.; Hu, S.; Du, X.; Wen, Q.; Zhong, X.-P.; Zhou, X.; Zhou, C.; Xiong, W.; Gao, Y.; Zhang, S. Vitamin B5 reduces bacterial growth via regulating innate immunity and adaptive immunity in mice infected with Mycobacterium tuberculosis. *Frontiers in immunology* **2018**, 365.
224. Zhao, Q.; Wang, J.; Yin, C.; Zhang, P.; Zhang, J.; Shi, M.; Shen, K.; Xiao, Y.; Zhao, Y.; Yang, X. Near-infrared light-sensitive nano neuro-immune blocker capsule relieves pain and enhances the innate immune response for necrotizing infection. *Nano letters* **2019**, *19*, 5904-5914.
225. Li, Y.; Xu, X.; Liu, X.; Li, B.; Han, Y.; Zheng, Y.; Chen, D.f.; Yeung, K.W.K.; Cui, Z.; Li, Z. Photoelectrons mediating angiogenesis and immunotherapy through heterojunction film for noninvasive disinfection. *Advanced science* **2020**, *7*, 2000023.
226. Tian, Y.; Li, Y.; Liu, J.; Lin, Y.; Jiao, J.; Chen, B.; Wang, W.; Wu, S.; Li, C. Photothermal therapy with regulated Nrf2/NF-κB signaling pathway for treating bacteria-induced periodontitis. *Bioactive Materials* **2022**, *9*, 428-445.
227. Yang, S.; Zhang, X.; Zhang, D. Electrospun chitosan/poly (vinyl alcohol)/graphene oxide nanofibrous membrane with ciprofloxacin antibiotic drug for potential wound dressing application. *International journal of molecular sciences* **2019**, *20*, 4395.
228. Ali, N.H.; Amin, M.C.I.M.; Ng, S.-F. Sodium carboxymethyl cellulose hydrogels containing reduced graphene oxide (rGO) as a functional antibiofilm wound dressing. *Journal of Biomaterials Science, Polymer Edition* **2019**, *30*, 629-645.
229. Sadat, Z.; Farrokhi-Hajiabad, F.; Lalebeigi, F.; Naderi, N.; Gorab, M.G.; Cohan, R.A.; Eivazzadeh-Keihan, R.; Maleki, A. A comprehensive review on the applications of carbon-based nanostructures in wound healing: from antibacterial aspects to cell growth stimulation. *Biomaterials Science* **2022**, *10*, 6911-6938.
230. He, Y.; Li, N.; Yang, S.; Tan, X.; Tang, L.; Yang, Q. Near-Infrared Molecular Photosensitizer Decorated with Quaternary Ammonium for High-Efficiency Photothermal Treatment of Bacterial Infections. *Chemosensors* **2023**, *11*, 164.
231. Tian, H.; Hong, J.; Li, C.; Qiu, Y.; Li, M.; Qin, Z.; Ghiladi, R.A.; Yin, X. Electrospinning membranes with Au@ carbon dots: Low toxicity and efficient antibacterial photothermal therapy. *Biomaterials Advances* **2022**, *142*, 213155.
232. Feng, Q.; Xu, J.; Zhang, K.; Yao, H.; Zheng, N.; Zheng, L.; Wang, J.; Wei, K.; Xiao, X.; Qin, L. Dynamic and cell-infiltratable hydrogels as injectable carrier of therapeutic cells and drugs for treating challenging bone defects. *ACS central science* **2019**, *5*, 440-450.
233. Dolinski, N.D.; Page, Z.A.; Callaway, E.B.; Eisenreich, F.; Garcia, R.V.; Chavez, R.; Bothman, D.P.; Hecht, S.; Zok, F.W.; Hawker, C.J. Solution mask liquid lithography (SMaLL) for one-step, multimaterial 3D printing. *Advanced Materials* **2018**, *30*, 1800364.
234. Ding, X.; Yu, Y.; Yang, C.; Wu, D.; Zhao, Y. Multifunctional GO hybrid hydrogel scaffolds for wound healing. *Research* **2022**, *2022*.
235. Federico, S.; Catania, V.; Palumbo, F.S.; Fiorica, C.; Schillaci, D.; Pitarresi, G.; Giammona, G. Photothermal nanofibrillar membrane based on hyaluronic acid and graphene oxide to treat Staphylococcus aureus and Pseudomonas aeruginosa infected wounds. *International Journal of Biological Macromolecules* **2022**, *214*, 470-479.
236. Zhang, H.; Zheng, S.; Chen, C.; Zhang, D. A graphene hybrid supramolecular hydrogel with high stretchability, self-healable and photothermally responsive properties for wound healing. *RSC advances* **2021**, *11*, 6367-6373.
237. Rosselle, L.; Cantelmo, A.R.; Barras, A.; Skandrani, N.; Pastore, M.; Aydin, D.; Chambre, L.; Sanyal, R.; Sanyal, A.; Boukherroub, R. An 'on-demand'photothermal antibiotic release cryogel patch: evaluation of efficacy on an ex vivo model for skin wound infection. *Biomaterials Science* **2020**, *8*, 5911-5919.
238. Mei, L.; Gao, X.; Shi, Y.; Cheng, C.; Shi, Z.; Jiao, M.; Cao, F.; Xu, Z.; Li, X.; Zhang, J. Augmented graphene quantum dot-light irradiation therapy for bacteria-infected wounds. *ACS Applied Materials & Interfaces* **2020**, *12*, 40153-40162.

Preprints (www.preprints.org) | NOT PEER-REVIEWED | Posted: 16 May 2023 doi:10.20944/preprints202305.1106.v1

239. Sun, Z.; Song, C.; Zhou, J.; Hao, C.; Liu, W.; Liu, H.; Wang, J.; Huang, M.; He, S.; Yang, M. Rapid photothermal responsive conductive MXene nanocomposite hydrogels for soft manipulators and sensitive strain sensors. *Macromolecular Rapid Communications* **2021**, *42*, 2100499.
240. Li, B.; Wang, W.; Zhao, L.; Yan, D.; Li, X.; Gao, Q.; Zheng, J.; Zhou, S.; Lai, S.; Feng, Y. Multifunctional AIE nanosphere-based "Nanobomb" for trimodal imaging-guided Photothermal/Photodynamic/Pharmacological therapy of drug-resistant bacterial infections. *ACS nano* **2023**, *17*, 4601-4618.

Disclaimer/Publisher's Note: The statements, opinions and data contained in all publications are solely those of the individual author(s) and contributor(s) and not of MDPI and/or the editor(s). MDPI and/or the editor(s) disclaim responsibility for any injury to people or property resulting from any ideas, methods, instructions or products referred to in the content.